

OCT 26 2004

## REPORT DOCUMENTATION PAGE

Form Approved  
OMB No. 0704-0188

Public reporting burden for this collection of information is estimated to average 1 hour per response, including the time for reviewing instructions, searching existing data sources, gathering and maintaining the data needed, and completing and reviewing the collection of information. Send comments regarding this burden estimate or any other aspect of this collection of information, including suggestions for reducing this burden, to Washington Headquarters Services, Directorate for Information Operations and Reports, 1215 Jefferson Davis Highway, Suite 1204, Arlington, VA 22202-4302, and to the Office of Management and Budget, Paperwork Reduction Project (0704-0188), Washington, DC 20503.

1. AGENCY USE ONLY (Leave blank)		2. REPORT DATE 25.Oct.04		3. REPORT TYPE AND DATES COVERED THESIS	
4. TITLE AND SUBTITLE RELAXATION OF KEVLAR BRAIDED CORDS				5. FUNDING NUMBERS	
6. AUTHOR(S) 2D LT FETTE RUSSELL B					
7. PERFORMING ORGANIZATION NAME(S) AND ADDRESS(ES) THE GEORGE WASHINGTON UNIVERSITY				8. PERFORMING ORGANIZATION REPORT NUMBER  CI04-650	
9. SPONSORING/MONITORING AGENCY NAME(S) AND ADDRESS(ES) THE DEPARTMENT OF THE AIR FORCE AFIT/CIA, BLDG 125 2950 P STREET WPAFB OH 45433				10. SPONSORING/MONITORING AGENCY REPORT NUMBER	
11. SUPPLEMENTARY NOTES					
12a. DISTRIBUTION AVAILABILITY STATEMENT Unlimited distribution In Accordance With AFI 35-205/AFIT Sup 1				12b. DISTRIBUTION CODE	
13. ABSTRACT (Maximum 200 words)					
<b>DISTRIBUTION STATEMENT A</b> Approved for Public Release Distribution Unlimited  <div style="font-size: 2em; font-weight: bold;">20041102 039</div>					
14. SUBJECT TERMS				15. NUMBER OF PAGES 71	
				16. PRICE CODE	
17. SECURITY CLASSIFICATION OF REPORT		18. SECURITY CLASSIFICATION OF THIS PAGE		19. SECURITY CLASSIFICATION OF ABSTRACT	
				20. LIMITATION OF ABSTRACT	

BEST AVAILABLE COPY

Standard Form 298 (Rev. 2-89) (EG)  
Prescribed by ANSI Std. Z39.18  
Designed using Perform Pro, WHS/DIOR, Oct 94

# **RELAXATION OF KEVLAR BRAIDED CORDS**

by

Russell Fette

B.S. in Engineering Mechanics, May 2003, US Air Force Academy

A Thesis submitted to

The Faculty of

The School of Engineering Management and Systems Engineering  
of The George Washington University in partial satisfaction  
of the requirement for the degree of Master of Science

June 28, 2004

Thesis directed by

Dr Shahram Sarkani

Professor of Engineering Management and Systems Engineering

## ABSTRACT

NASA uses Kevlar Aramid Fiber in constant strain applications in the form of braided cord. Questions about its behavior in load relaxation with variables including time, temperature, humidity, initial and re-tensioning loads are probed by this report, beginning with a literature review. Testing was performed at NASA Goddard SFC to attempt to resolve unanswered questions. The results are demonstrative of three important findings:

- The first is that the *initial relaxation phase is generally log-linear*.
- The second finding of this phase of testing is an *average relaxation rate ( $\beta$ ) of  $-0.0151 \text{ \%}/\log(t)$  with a standard deviation of  $\pm 0.0021$ .*
- The third finding is that the primary relaxation phase represents a 41% higher relaxation rate than the secondary phase. Kevlar exhibits load relaxation at a rate ( $\beta$ ) of approximately  $-0.0110 \pm .0027 \text{ \%}/\log(t)$  *after preconditioning* or primary relaxation.

Kevlar's secondary relaxation generally fits a log-linear relaxation model as expected from the literature. The data experienced a short recovery period after reloading and transferring the load to the load cell, which may be traced to material, and/or environmental effects. In general, the data exhibited a wide scatter and several highly erratic responses, which indicate that precisely modeling this material may be impossible.

## ABSTRACT

NASA uses Kevlar Aramid Fiber in constant strain applications in the form of braided cord. Questions about its behavior in load relaxation with variables including time, temperature, humidity, initial and re-tensioning loads are probed by this report, beginning with a literature review. Testing was performed at NASA Goddard SFC to attempt to resolve unanswered questions. The results are demonstrative of three important findings:

- The first is that the *initial relaxation phase is generally log-linear*.
- The second finding of this phase of testing is an *average relaxation rate ( $\beta$ ) of  $-0.0151 \text{ \%}/\log(t)$  with a standard deviation of  $\pm 0.0021$ .*
- The third finding is that the primary relaxation phase represents a 41% higher relaxation rate than the secondary phase. Kevlar exhibits load relaxation at a rate ( $\beta$ ) of approximately  $-0.0110 \pm .0027 \text{ \%}/\log(t)$  *after preconditioning* or primary relaxation.

Kevlar's secondary relaxation generally fits a log-linear relaxation model as expected from the literature. The data experienced a short recovery period after reloading and transferring the load to the load cell, which may be traced to material, and/or environmental effects. In general, the data exhibited a wide scatter and several highly erratic responses, which indicate that precisely modeling this material may be impossible.



## Relaxation of Kevlar Braided Cords

A Thesis Presentation by  
Russell Fette  
22 Sep 2004



## Outline

- Background
- Fundamentals and Models
- Testing
- Results and Conclusions
- Future Direction



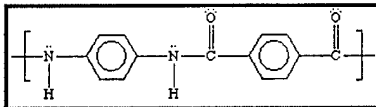
## Background

### Reactive Motivations

- EOS Satellite Series

### Proactive Motivations

- Future Solar Array Designs
- Industry and Science



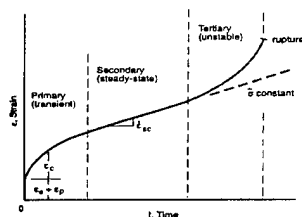
## Background

- Kevlar Aramid Fiber (K49)
- Kevlar is a highly crystalline polymer
  - LCP spun into a fiber
  - Molecules aligned with shear forces
  - High modulus, high strength to weight
  - Low time and temperature degradation
- A study of time dependent behavior
- Timeline: 5 Aug 2003 – 28 Jun 2004



## Fundamentals

### Time Dependant Behavior



## Fundamentals

### Classical Polymer Relaxation Theory

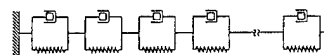


Figure 5: Generalized Maxwell Model [Ferry, 1980].

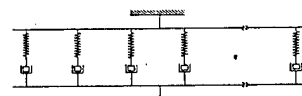


Figure 6: Generalized Voigt Model [Ferry, 1980].



## Fundamentals

### Boltzmann Superposition Principle

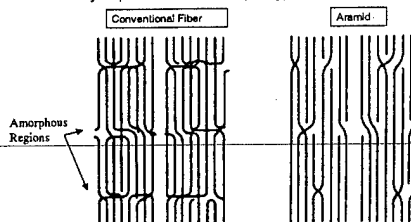
- Assumption of Linear Viscoelasticity
- "The effects of mechanical history are linearly additive"
- Advantages of this simplification
  - Creep and Relaxation can be directly compared
  - Identical creep/relaxation regardless of strain/stress



## Modeling Kevlar

### Comparison of Crystalline Structure

- Nearly 100% crystalline
- Likely departure from LVE (Ferry)



## Modeling Kevlar

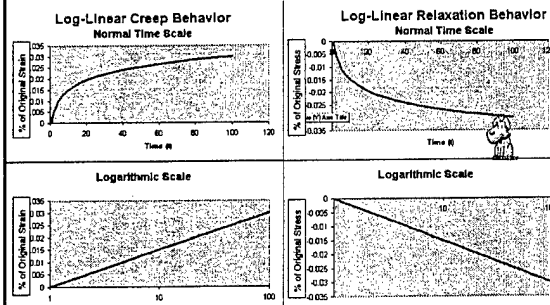
### Purely Mathematical Approach

- Lafitte rejects 4 component Maxwell models for a Log-Linear Creep model
- Wang 1992, Duband 1992, Riewald 1988, Erickson 1985, Blades 1983
- Models for Stress Relaxation:
  - Power Law models
  - Logarithmic Models



## Modeling Kevlar

### Graphing the Mathematical Approach



## Modeling Kevlar

### The Working Assumption

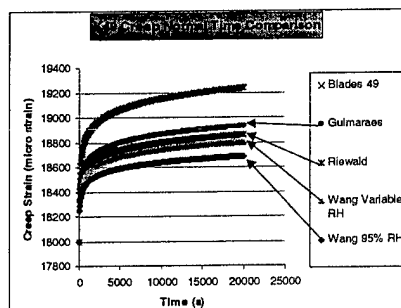
$$\epsilon(t) = \beta \log_{10}(t) + \epsilon_1 \quad t > 0 \quad (1) [\text{Guimaraes, 1992}]$$

$$\sigma(t) = \beta \log_{10}(t) + \sigma_1$$



## Modeling Kevlar

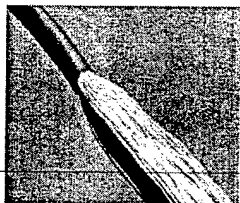
### Literature Summary





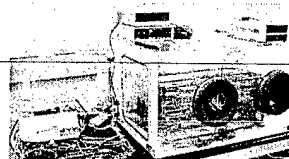
## Modeling Kevlar Relevant Factors

- Preconditioning
  - Load (Primary vs. Secondary phases)
  - Temperature
  - Humidity
- Type
  - Weave, Braid, twist
  - Differences: Boone, Coskren, Erickson
  - Same: Cortland, Guimaraes



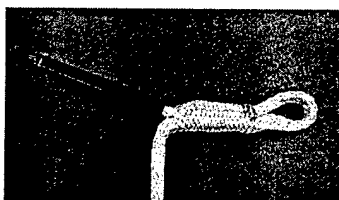
## Modeling Kevlar Relevant Factors

- Temperature
  - CTE
  - Accelerated Relaxation
- Initial Load
  - LVE vs. NLVE
- Humidity
  - CME
  - Accelerated Relaxation
- Pressure
- Recovery



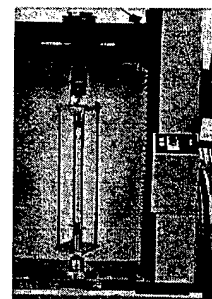
## Experimental Setup Specimen Buildup

- Product – Formation – Testing



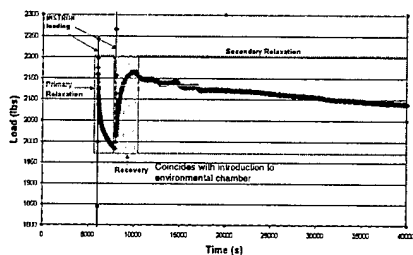
## Experimental Setup Equipment and Processes

- Relaxation Cell
- Strain Gauges
- Computers
- Environmental Chamber
- Preconditioning and Control
- Loading Process



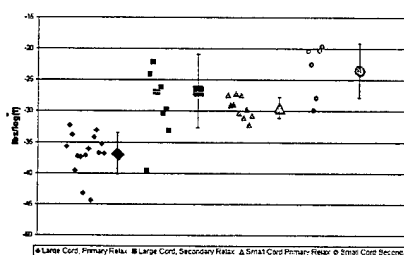
## Results Typical Analysis

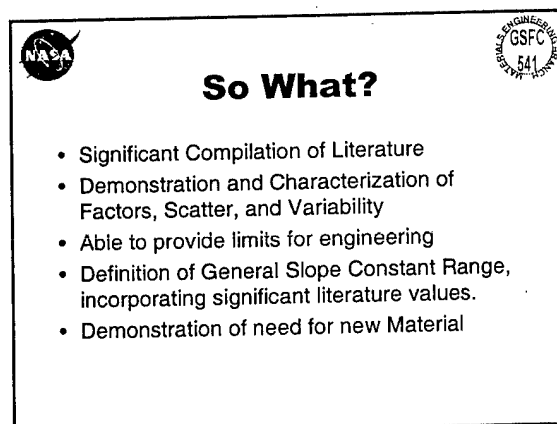
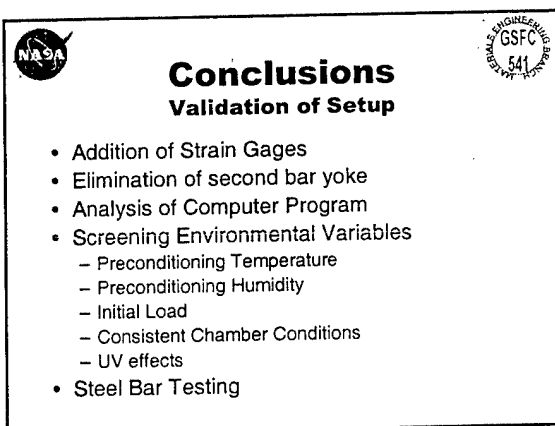
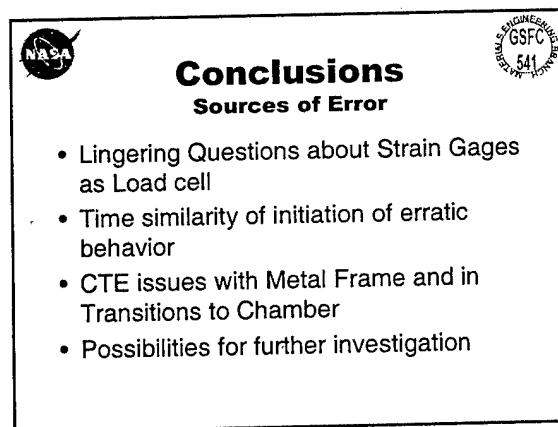
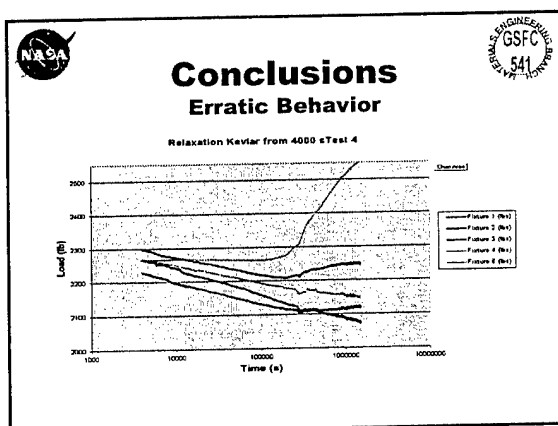
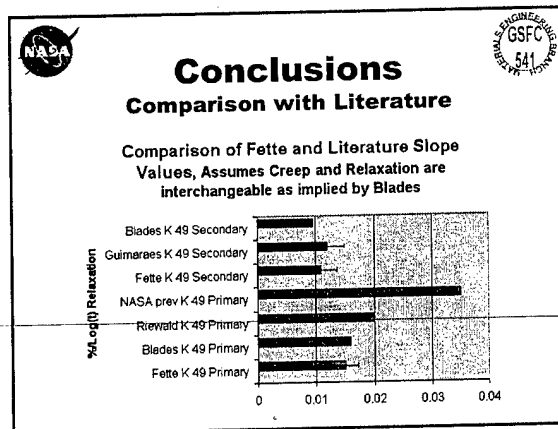
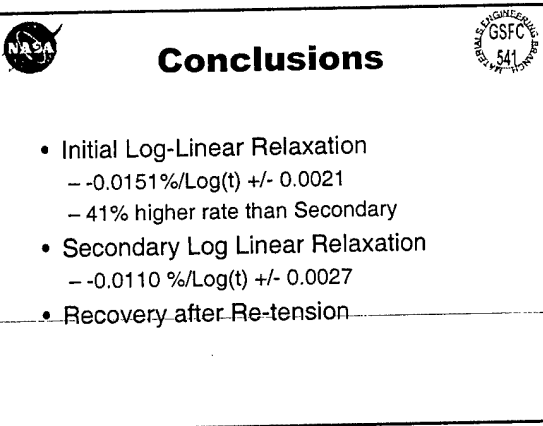
Summary of Testing cycle



## Results Summary

Summary and Comparison of Valid Slope Constants







## Future Direction

- Vectran Holds Promise
- Manufacturer's Claim of Zero Creep is being proved wrong
- Goal is a consistent, predictable, low creep/relaxation material



## Questions



**U.S. AIR FORCE**

## ACKNOWLEDGEMENTS

Special thanks to the following people. Mr. David Puckett, Mr. Michael Viens, Mr. Dewey Dove, Mr. Douglas Bentley, Mr. Jerry Sterling.

"The views expressed in this article are those of the author and do not reflect the official policy or position of the United States Air Force, Department of Defense, or the U.S. Government."

## TABLE OF CONTENTS

	<u>Page</u>
Abstract	ii
Acknowledgements	iii
Table of Contents	iv
List of Figures	vi
List of Tables	vii
List of Acronyms	viii
Glossary	ix
Chapter 1 Introduction	1
1.1 Orientation	1
1.2 Fundamentals	3
1.3 Current Models	6
Chapter 2 Background and Problem Statement	8
2.1 General Model Shape	8
2.2 Preconditioning by Loading	11
2.3 Types of Products Studied	11
2.4 Temperature Variable	13
2.5 Initial Load Variable	15
2.6 Humidity Variable	16
2.7 Pressure Variable	19
2.8 Recovery Variable	19

Chapter 3	Results and Analysis	20
3.1	Specimen Buildup	20
3.2	Test Setup	23
3.3	Preconditioning and Loading	26
3.4	Data Acquisition	29
3.5	Data Analysis	29
3.6	Results	32
Chapter 4	Conclusion	35
4.1	Primary Relaxation	35
4.2	Secondary Relaxation	35
4.3	Sources of error	37
Chapter 5	Future Direction	41
References		42
Appendix A.	Kevlar 49 Property Summary	
Appendix B.	Literature Review Mode Comparison	
Appendix C.	Power vs. Semi-Log Comparison	
Appendix D.	Equipment List	
Appendix E.	Kevlar Relaxation Test Plan	
Appendix F.	Collection of Test Plots	

## LIST OF FIGURES

	<u>Page</u>
Figure 1.1     Chemical Structure of Kevlar.....	1
Figure 1.2     Depiction of Braided Cord and Parallel Lay Rope.....	1
Figure 1.3     Strain vs. Time Behavior of Creep.....	4
Figure 1.4     Transient Creep Model.....	4
Figure 1.5     Generalized Maxwell Model.....	5
Figure 1.6     Generalized Voigt Model.....	5
Figure 1.7     Conventional Fiber vs. Para-aramid Fiber Structure.....	6
Figure 1.8     Master Sheet of Literature Review Model Comparison.....	7
Figure 2.1     Relaxation Comparison from Blade's Equation to NASA Experiments.....	10
Figure 2.2     Anatomy of a Braided Cord.....	12
Figure 2.3     Boltzmann Superposition for Creep.....	16
Figure 2.4     Moisture Properties of Kevlar Aramid Fiber.....	18
Figure 2.5     Load and Relative Humidity Versus Time Recovery of Kevlar.....	18
Figure 3.1     Bury Splice of Kevlar Specimen.....	20
Figure 3.2     Dimensioned Picture of Test Specimen.....	21
Figure 3.3     Relaxation Cell Depiction.....	23
Figure 3.4     Cast Eye Bolts.....	24
Figure 3.5     Environmental Chamber and Kevlar Cells.....	25
Figure 3.6     Preconditioning and Loading in the INSTRON.....	27
Figure 3.7     Summary of Testing Cycle.....	30
Figure 3.8     Summary and Comparison of Valid Slope Constants.....	32
Figure 3.9     Display of Erratic Kevlar Behavior.....	34

Figure 4.1	Response of Kevlar 49 to Temperature Changes.....	39
Figure 4.2	Slope Constant Comparison.....	40

### LIST OF TABLES

		<u>Page</u>
Table 3.1	Summary of Strength Testing.....	21
Table 3.2	Testing Conditions for Kevlar.....	28
Table 3.3	Summary of all Slope Constants.....	33
Table 3.4	Average Slope Constants.....	34

## LIST OF ACRONYMS

541	Material's Engineering Branch Code
B49	Braided Kevlar 49
CME	Coefficient of Moisture Expansion
CTE	Coefficient of Thermal Expansion
EOS	Earth Observing Satellite
gpd	grams per denier
GSFC	Goddard Space Flight Center
HMPE	High Modulus Poly-Ethylene
LCP	Liquid Crystalline Polymer
LVE	Linear Visco-Elastic
MEB	Materials Engineering Branch
NASA	National Air and Space Association
NLVE	Non-Linear Visco-Elastic
PBO	Poly [p-phenylene-2, 6-benzobisoxazole]
SFC	Space Flight Center
T <sub>g</sub>	Glass Transition Temperature
USAF	United States Air Force
UV	Ultra-Violet light

## **GLOSSARY**

**Denier** -A unit of fineness for rayon, nylon, and silk fibers, based on a standard mass per length of 1 gram per 9,000 meters of yarn [Dictionary, 2000].

---

## CHAPTER 1

### INTRODUCTION

#### 1.1 Orientation:

KEVLAR is the popular trade name for Poly(p-phenylene terephthalamide) [Mark, 1996]. It is an aromatic polyamide fiber, or an aramid [Mark, 1996] created by the DuPont in 1971 using a revolutionary process where a liquid crystalline polymer was spun into a fiber using shear forces that caused near perfect molecular orientation [Kevlar, 2003]. Its chemical structure is depicted in Figure 1.1 below, and a property summary is in Appendix A.

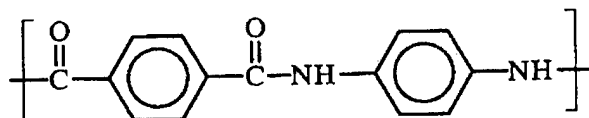


Figure 1.1: Chemical Structure of Kevlar [Mark, 1996].

High modulus, high strength and strength to weight ratio, and relatively low time and temperature degradation led to its rapid employment in composites, and many classic fiber products (ropes, cords, yarns, fabrics, etc...). There are many forms of aramid fibers in existence, and several forms of Kevlar. This study focused on Kevlar 49 due to its direct correlation with flight hardware for the EOS (Earth Observing Satellite) series.

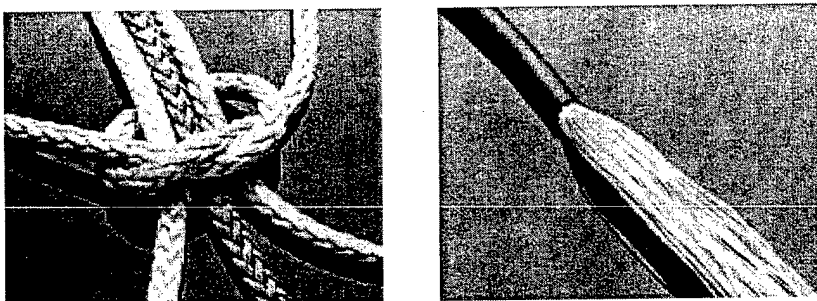


Figure 1.2: Depiction of Braided Cord and Parallel Lay Rope [Cortland, 2003].

This study is intended to probe the response of Kevlar 49 in tensile fiber applications (primarily in the form of braided cord) to stress relaxation under variations in environmental conditions. The original reactive motivation for the study comes from difficulties encountered in accurately predicting the relaxation behavior of loops of Kevlar 49 braided cord used to tie down the solar arrays on satellites. As many as 13 loops would hold these arrays in folded position for launch, and would be cut by thermal knives once in orbit. However, excessive relaxation could result in enough loss of tension to disrupt the cuts [NASA, Apr 2000]. The cords are often exposed to varying environmental conditions while awaiting launch, and in the transition from sea level to the vacuum of space. Insufficient information is available in literature to make accurate predictions such as might be possible for metal relaxation.

This investigation was performed at a macroscopic level with the end goal of producing an equation or set of equations that can be used to accurately predict the stress relaxation behavior of Kevlar over time, taking into account environmental effects. Specific understanding of the molecular processes should not be slighted, as it is vital to an exact formulation of such an equation for all cases. There have been prolific studies (Allen, Erickson, Habeger, Kunugi, Rogozinsky, Wang, Wortmann and others referenced in their works) on the relaxation of aramid fibers that probed this microscopic perspective, with no definitive or complete model. Additionally, there is a decided lack of an in-depth, practical model for those currently employing the fiber. Studies at NASA, and elsewhere do not agree in their conclusions. Therefore, in a proactive sense this investigation is intended to provide NASA, and industry in general with better understanding of Kevlar relaxation in the form of braided cord.

## 1.2 Fundamentals:

The time dependent load behavior of materials is characterized by creep and stress relaxation. Creep describes a material that under a constant load experiences an increasing total strain with time. Stress relaxation refers to a material that is initially strained to a fixed dimension, and then over time, the stress within the material decreases. This phenomenon is observed to some degree in almost every engineering material with the exception of a perfect single crystal. There is an activation temperature required to initiate this time dependent relaxation of the material, which may be seen as primary driver of the process. Other factors may have an effect on relaxation such as moisture, pressure, and the degree of the applied strain or load. All of these vary greatly with each material and the underlying molecular processes are also numerous. Metallic materials in general relax very slowly and require high activation energies as compared to polymers. Polymers display viscoelastic properties where their behavior can be described as a mix between a pure solid (governed by Hooke's Law) and a pure liquid (governed by the laws of fluid mechanics). Maxwell models consisting of a series of springs and dashpots are often used to describe (at least conceptually) the relaxation of polymers over time [Askeland, 1994; Ferry, 1980].

A classical model of the creep behavior of a material has three stages of strain vs. time behavior of creep (constant load). The first stage consists of the initial elastic and plastic effects of loading, and an initially high, but rapidly decaying creep rate. This is followed by steady state creep in stage two where the rate is linear with time, and concludes with tertiary creep where the creep rate rapidly accelerates and ends in failure.

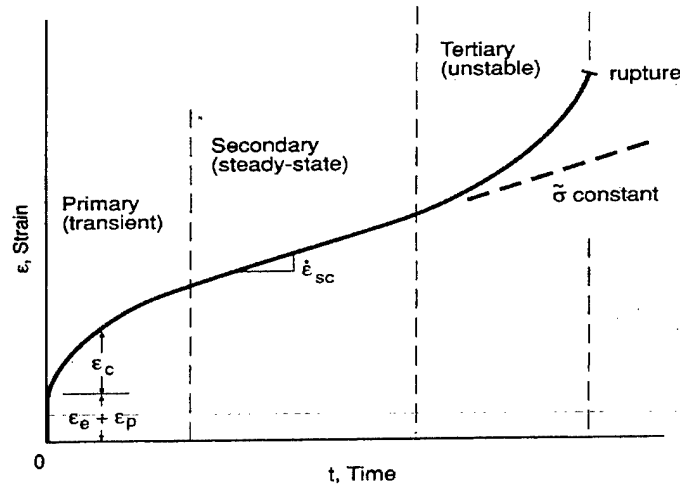


Figure 1.3: Strain vs. Time Behavior of Creep [Dowling, 1999].

In reference to Kevlar, Erickson states that “The creep is always transient and no evidence of either a steady state creep component or a third stage was observed” [1985]. Guimaraes also observes a lack of transition from primary to secondary creep, but a universal response leading to tertiary creep and failure [1992]. A basic model for transient creep is presented below.

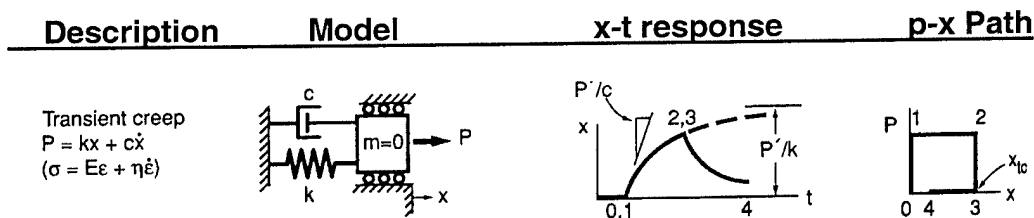


Figure 1.4: Transient Creep Model [Dowling, 1999].

Where:

$P$  = force, which is analogous to stress ( $\sigma$ )

$x$  = displacement, which is analogous to strain ( $\epsilon$ )

$k$  = spring constant, which is analogous to the Elastic component ( $E$ )

$c$  = dashpot constant, which is analogous to the Viscous component ( $\eta$ )

The disagreement over the reaction near to failure may be caused by the differences in product tested (fibers vs. rope) and are immaterial to this study which assumes that initial stresses are below that required to result in fiber failure due to creep or relaxation during the employment time.

In classic polymer relaxation theory, the time dependant behavior is governed by highly developed equations often based on Maxwell or Voigt models (made up of springs and dashpots) and governed by a spectrum of relaxation times for the material. [Ferry, 1980; Schmitz, 1995]. These generalized models are shown below, and it can be observed that the transient creep model depicted above is identical to a single Voigt element.

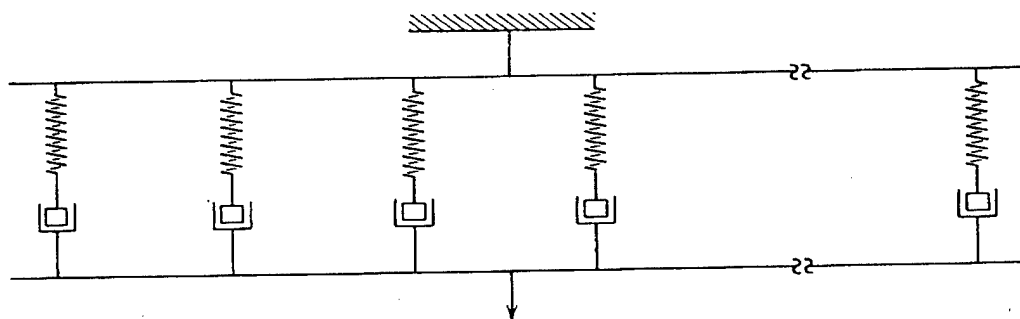


Figure 5: Generalized Maxwell Model [Ferry, 1980].

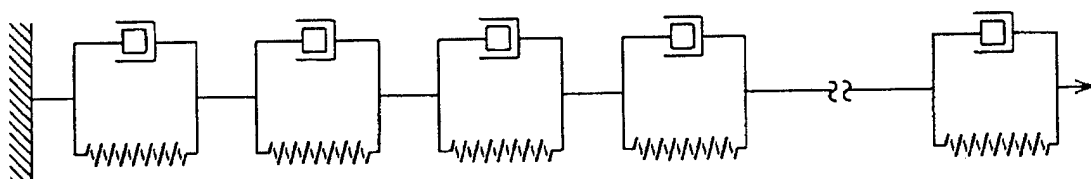


Figure 6: Generalized Voigt Model [Ferry, 1980].

To describe real systems, these models become very complicated. Under the theory of Linear Viscoelasticity, the Boltzmann superposition principle applies which states that the effects mechanical history are linearly additive [Ferry, 1980]. There are many other advantages to working under the conditions of linear behavior, such as the ability to compare creep and

relaxation behavior directly. This condition of linearity can also be understood as stating that the materials will creep/relax identically, regardless of the degree of stress/strain [Ferry, 1980].

Kevlar aramid fiber is nearly 100% crystalline [Erickson, 1985], leading to a high likelihood of a rapid departure from the Linear Viscoelasticity Theory used to describe and analyze most polymers [Ferry, 1980]. It has little or no amorphous regions that generally relate to classic viscoelastic theory. The chains that in amorphous polymers entangle in defect zones often go straight through into the next crystal [Zachariades, 1983]. This is pictured in Figure 1.7 below.

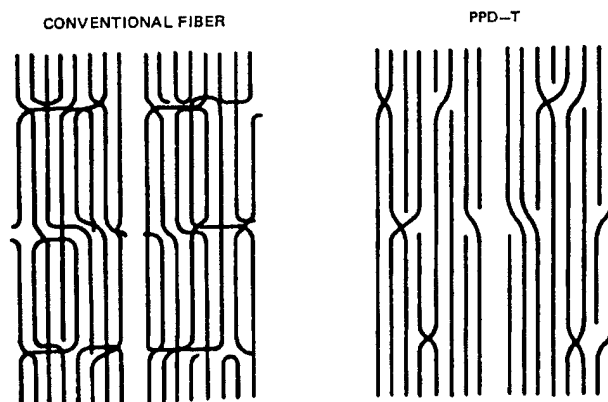


Figure 1.7: Conventional Fiber vs. Para-aramid Fiber Structure [Zachariades, 1983].

Lafitte rejects the use of four component Maxwell models in describing Kevlar, opting for a purely mathematical approach [1985]. In fact, almost every study found in this literature review also rejected such mechanical models and used a simpler mathematical form than the spring/dashpot models to describe the basic behavior of Kevlar. Their methods become increasingly complicated as additional variables are added such as temperature.

### 1.3 Current Models:

A summary of all significant models for Kevlar fiber time dependant behavior is contained in the excel spreadsheet entitled "Literature Review Model Comparison." Its

summary sheet is attached as Appendix B. Only Blades (in Zachariades) gave a model for stress relaxation [1983], which he described as following a similar process as creep. Therefore, the comparison of the creep models offered by other researchers is not without merit. There is general agreement in the shape of functions, and under certain temperature and initial strain conditions, the curves overlap. These variables can be changed on the Master sheet of the spreadsheet and the updates in the resulting functions for each model will be represented in the graphs below. A screenshot of the Master sheet is shown below.

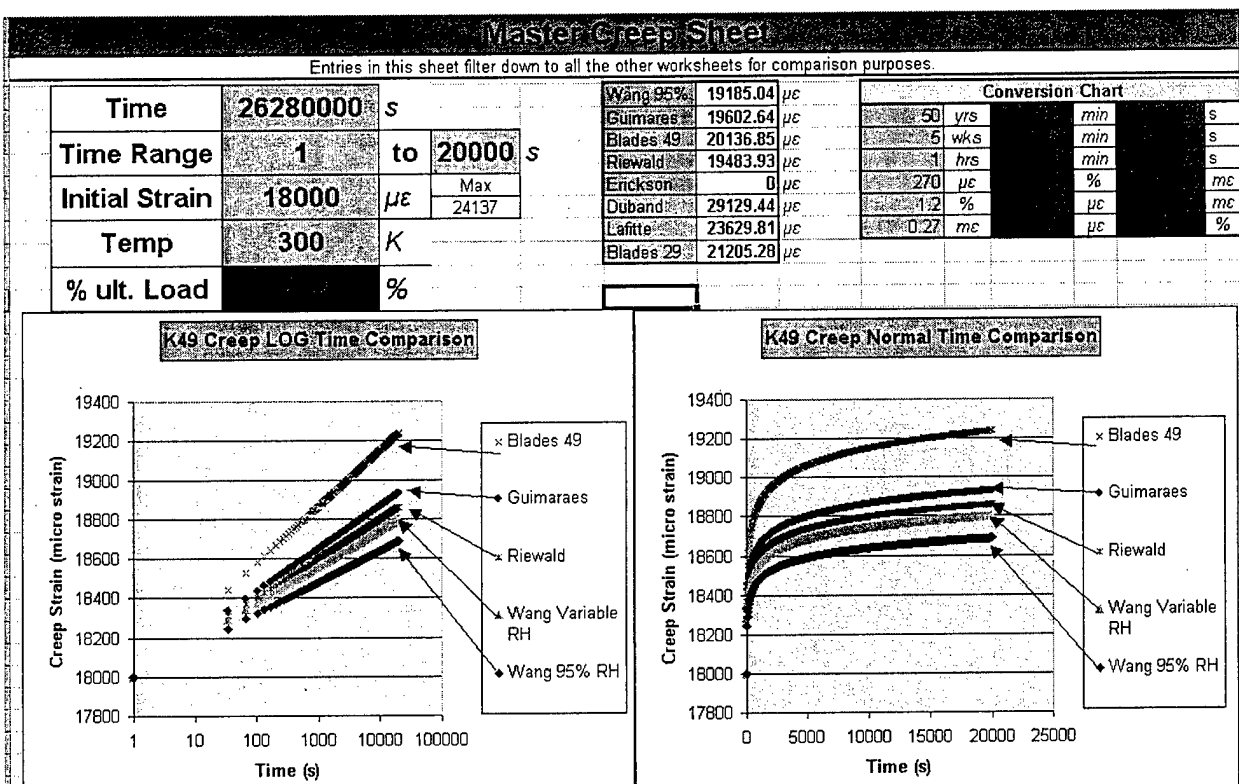


Figure 1.8: Master Sheet of Literature Review Model Comparison.

Unfortunately, there is no definite agreement amongst the reports. This is attributed to the lack of consistent test conditions including type of material (fiber, yarn, rope), temperature, humidity, initial strain, time, and grip mechanism. Furthermore, some studies consider and vary these conditions, but none make a concerted effort to summarize and develop a master model.

## CHAPTER 2

### BACKGROUND AND PROBLEM STATEMENT:

#### 2.1 General Model Shape:

There is a general (though not universal) consensus throughout a survey of available literature that the creep of Kevlar aramid fibers can be modeled as a logarithmic creep rate, which appears linear on a semi-log plot (log time on independent axis). Most of these studies were performed on fibers, although the one study found on rope indicated an identical response. This can be represented in equation one below.

$$\epsilon(t) = \beta \log_{10}(t) + \epsilon_1 \quad t > 0 \quad (1)[\text{Guimaraes, 1992}]$$

Erickson's extensive "Creep of Aromatic Polyamide Fibers" noted that "There was no indication any of the tests of a systematic departure from logarithmic creep"[1985]. Other reports using purely logarithmic creep to define the behavior of aramid fibers include: Wang 1992, Duband 1992, Riewald 1988, Erickson 1985, and Schaeffgen in Zachariades 1983. Lafitte notes a secondary creep mode in Kevlar 29, which he says can be neglected due to relatively minor contributions [1985]. This secondary creep mode in Kevlar 29 is also noted in Yang's book on Kevlar, and noted as a difference between K29 and K49 [1993]. Erickson claims to see no evidence of either tertiary or steady state creep, observing only the transient creep region [1985].

However, the focus of this study is primarily on stress relaxation, which may not be predicted exactly by creep. Three references in Allen noted that the stress relaxation of Kevlar has been represented by power law models [1989]. One of the references noted is Schaeffgen in Zachariades who actually uses a logarithmic decay and finds the constant for such a relationship to be identical to that of the creep constant, implying similar processes [1983]. The

only variance is that the constant (Beta in these examples) is negative for stress relaxation.

Mathematical analysis will quickly show that a power law when converted to logarithmic form is not of the same form as the models proposed for logarithmic creep.

*Power Law*  $\sigma(t) = \sigma_1 t^\beta$

*Take the Logarithm*  $\text{Log}(\sigma(t)) = \text{Log}(\sigma_1) + \beta \text{Log}(t)$  (2)

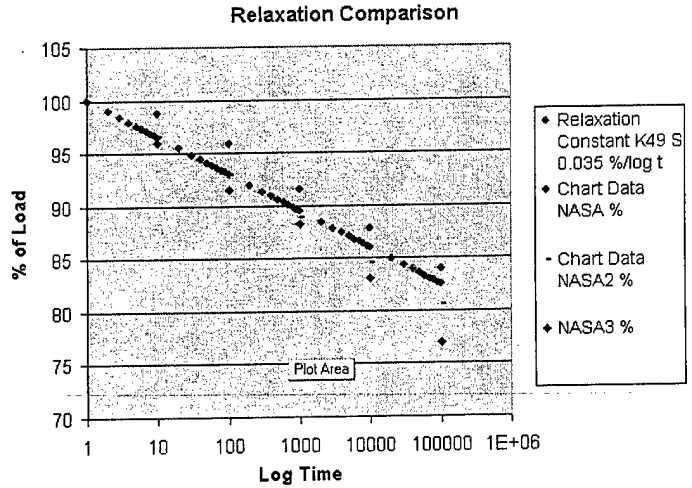
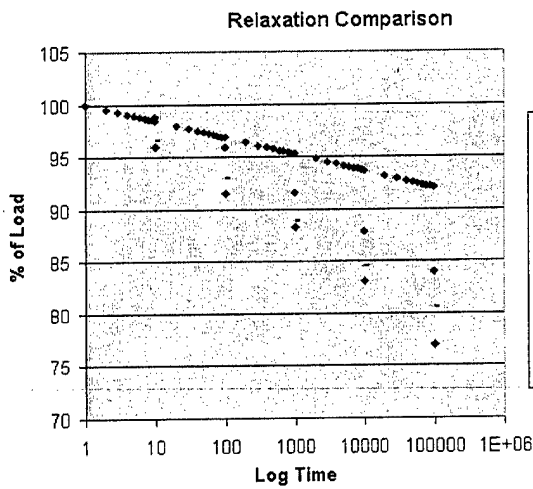
vs.

*Model for Logarithmic Creep*  $\sigma(t) = \sigma_1 + \beta \text{Log}(t)$  (3)

*Note that strain may be substituted for stress:  $\sigma \approx \epsilon$*

Further investigation shows, however, that both models can be used to describe the same behavior in very similar fashion, though requiring different constants. An excel analysis is included as Appendix C in support of this statement. The summation of this evidence leads to the hypothesis that the stress relaxation behavior of Kevlar can be adequately and precisely modeled with a power law relationship or semi-logarithmic decay assuming the correct constants, which may vary under different conditions.

The majority of experimentation with Kevlar relaxation in the form of creep has chosen to use the semi-logarithmic relationship, and the only reported model for stress relaxation also uses this model. This model was compared to actual stress relaxation test results from NASA. It was found that the model fit very well under cursory comparisons, although the relaxation constant given for Kevlar 49 needed to be changed significantly. This is not a detriment to the model, but only an indication of the wide range of variance in the relaxation constant that may be seen due to the many variables encountered. A graphical depiction of this analysis is shown below, and the constants are shown in the legend.



NASA 1 and 2 represents the S/N 16 and 10 (respectively) curves from Figure 3 in the May 4, 1998 report without a preload. NASA3 represents Figure 5, 10" specimen from the Sept 20 1999 report, where the specimen was preloaded to 500 lbs for 1/2 hr and then allowed to relax at ambient conditions. Values were approximated from printed report charts by hand. The reported value of 0.016 did not fit actual data.

Figure 2.1: Relaxation Comparison from Blade's equation to NASA experiments.

Therefore, the following equation is proposed, where Beta is assumed to be negative.

$$\sigma(t) = \beta \log_{10}(t) + \sigma_1 \quad t > 0 \quad (4)$$

$\sigma(t)$  = Stress at time  $t$

$\beta$  = Constant

$t$  = time

$\sigma_1$  = Stress at  $t = 1$

## **2.2 Preconditioning by Loading:**

After an initial creep or stress relaxation, given time to relax equal to or less than the initial straining time, Kevlar shows a different constant  $\beta$ , at a typically lower creep or stress relaxation rate. 60% has been quoted as an approximation of the difference in rate [Guimaraes, 1992]. After the initial drop, repeated loading cycles leave the slope constant the same.

Also, there is a decided difference in the response of Kevlar end products such as yarn, lay rope, and braided cord when compared to fiber. J.D. Boone doing tests on parachute cord noted it as early as 1975. The simpler yarn he tested had a steeper slope and was more predictable [Boone, 1975]. However, Cortland Cable Company, who manufactured the actual braided cord used here at NASA for testing, noted that the material tends to follow the fiber relaxation properties if pre-stressed initially to at least twice it's design load, and allowed to relax to its desired load [2003]. A study on parallel-lay aramid rope also noted the necessity of pre-tensioning to 60% of the nominal breaking load in order to remove "any possible initial disorientation of the fiber lay" [Guimaraes, 1992], and also has the effect of reducing creep and possibly relaxation [Guimaraes, 1992].

## **2.3 Types of Products Studied:**

It has been demonstrated that there are ideal configurations for yarn twist (1.1 twist multiplier) and braided cords [Coskren, 1975; Erickson, 1981]. Also, UV rays are known to cause degradation in Kevlar as reported in the DuPont product manual. Noticeable browning has been seen in the fibers stored under fluorescent lighting at NASA, and the bright gold color can still be seen on the inside of the cord. Care must be taken to eliminate any effects this variable may produce. A picture of both braided cord and parallel lay rope such as studied by

Guimaraes are included on Page 1, Figure 1.2. A diagram showing the basic construction of a braided cord such as that used in this study is below.

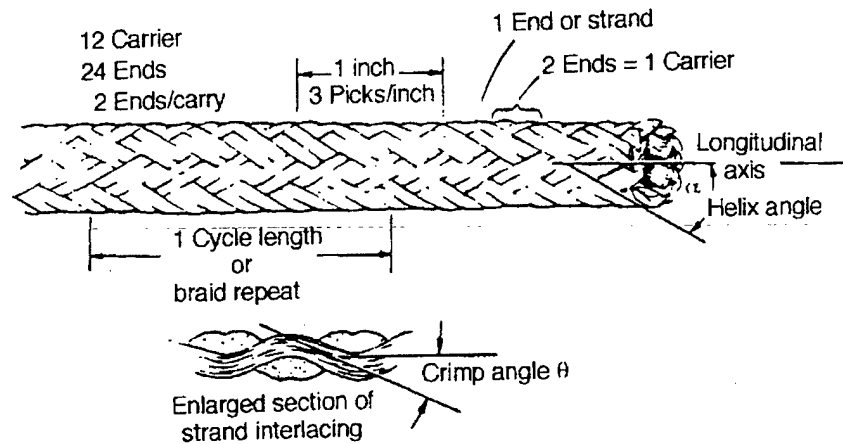


Figure 2.2: Anatomy of a Braided Cord [Yang, 1993].

The specific product to be studied is a single braid cord. It is produced by Cortland Cable, and designated B49 16x1420x6 and B49 16x1420x4. This refers to *Braided Kevlar 49* material in a *16-strand braid* of *1420-denier yarn* with either *6 or 4 lines* of this yarn per strand in the braid [Bently, 2003]. The x6 version therefore has 50% more material than the x4 variety left over from work. These cords may be referred to as x6 cord and x4 cord, referring to the large and small diameter cords we tested. These cords are used because they are the specific variety used for the EOS satellite series.

An interesting side note pertains to discrepancies noted in the theoretical extension to failure and the theoretical strength as opposed to actual values seen by NASA in braided cord experimentation. Studies have been performed that demonstrate failure due to creep, with failure time decreasing with increased load [Boone, 1975; Bunsell, 1975]. The fiber can be expected to fail at or near it's elongation at failure, 2.8% [Yang, 1993]. The braided cord tested by NASA at ½ turn around a pulley in a loop configuration failed due to creep at an average

elongation of 6.2 %. This was calculated by dividing the extension at failure by  $\frac{1}{2}$  the loop circumference from the values reported in table 4 of the "Strength Testing of Kevlar Cord used in the EOS Solar Array Deployment Mechanism" Report, August 31, 2000. Insufficient background for these experiments has been studied to account for this apparent discrepancy.

Also, Yang reports strength for Kevlar 49 fiber of 23 gpd [1993]. The braided cord used in the strength testing report by Mr. Viens, August 31, 2000 reports the highest average ultimate strength to be 38.9 kN in a loop configuration, therefore, 19.45 kN per diameter of braided cord [NASA, Aug 2000]. The denier of this cord is 136,320 (as calculated from it's manufacturer's designation 16x1420x6). Multiplying this by the Yang value and converting from g to kN gives a value of 30.73 kN. This represents a 36.7 percent reduction in strength in the braided cord. There are many different variables which could have caused this such as the splice, loop configuration, temperature, humidity, stress history, fiber interactions, etc... Such a large discrepancy sheds doubt on the feasibility of comparing different types of Kevlar products, in spite of the positive information reported by Cortland Cable and the Guimaraes rope study.

#### **2.4 Temperature Variable:**

Kevlar fibers undergo severe degradation above 500 C [Yang, 1993]. They do not melt, but will begin to decompose at 427 C [Kevlar, 2003]. Lafitte observed a rapid decrease in the Young's modulus and strength of the fiber at 300 C [1985]. Exposure to arctic and cryogenic temperatures shows no drastic embrittlement as low as -196 C [Kevlar, 2003]. This gives the widest scale of temperatures that Kevlar is likely to be employed in. Kevlar's use in the vacuum of space by NASA and cryogenic applications such as studied by Duband motivate us to maintain the lower temperature as a study bound.

There is no consensus on what the glass transition temperature is for Kevlar, if there is one at all. This transition refers to the temperature where the CTE undergoes an abrupt change in the region where the modulus is changing from a glass to a rubber-like behavior [Aklonis, 1983]. Either of these changes (in modulus or CTE) can be used to define the transition temperature, which can be a cause of discrepancy in the reported values [Montoya, 2003]. Yang reports a  $T_g$  of 375 C [1993], Mark reports 344 C [1996] and Riewald says that there is no detectable glass transition temperature [1988].

Temperature can be demonstrated as a driving factor for creep in crystalline solids and polymers. Two studies that examined the effects of temperature on creep have proposed the Arrhenius equation as a model for the effects of temperature on creep, with an array of apparent activation energies, varying with load [Erickson, 1985] and relative humidity [Wang, 1992].

Therefore, the following equation from Wang [1992] is proposed for the purely thermal contribution to the relaxation of Kevlar fiber.

$$\overline{\beta}_i = A_i \frac{-E_a^{(i)}}{RT} \quad (6)$$

Where

i = represents the variation of these terms with humidity and other variables

$\overline{\beta}_i$  = Average value of the relaxation rate

$A_i$  = Proportionality constant

$E_a^{(i)}$  = Apparent activation energy

R = gas constant (8.33 J/mol K)

T = absolute temperature (K)

There is a known and measured negative Coefficient of Thermal Expansion for Kevlar of  $-4.9$  [Kevlar, 2003]. Studies performed at NASA Goddard SFC (April 2003) have found a negative CTE of  $-6.67 \pm 0.72 \mu\text{m/m/C}$  from  $-130^{\circ}\text{C}$  to  $60^{\circ}\text{C}$  [NASA, Apr 2003]. Yang reports values that vary from  $-4 \mu\text{m/m/C}$  to  $-5.7 \mu\text{m/m/C}$  [1993]. However, these tests were performed at room temperature. It is known that the CTE will vary over a large temperature range. Possible differences in the NASA vs. DuPont data include: Relative Humidity (65% at DuPont, ambient/uncontrolled at NASA), Twist of strands (0 twist at DuPont vs. possible 1.1 yarn twist from braided cord at NASA), UV degradation of fibers in storage at NASA (noticeable browning of cordage has been noted over several years of storage), and degree of applied load (0.2 gpd at DuPont vs. 0.0 gpd at NASA). Further testing may be motivated by these discrepancies to formulate a good predictive model. This must not only be taken into account in a final model, but the effects it has by straining the material under changing temperatures may also be significant, and thus the interrelationships should be examined.

## **2.5 Initial Load Variable:**

There is not a general agreement on the contribution of load to Kevlar's creep rate. Habeger describes it as insensitive while Lafitte goes so far as to quantify it in his mathematical models. Most investigators reporting actual prediction models have disregarded it as insignificant, but do not give specifics on the range over which it was studied or why it was rejected. Erickson notes the appearance of a relationship, but did not investigate it further. While Kevlar may not be extremely sensitive in creep or relaxation to the applied load, there is not enough information to presuppose a lack of significant response.

Guimaraes in his parallel lay rope study notes that the primary advantage of disregarding the effects of initial load is the material can be modeled as a Linear Viscoelastic

material [1992]. In this case, the Boltzmann superposition principle applies and the material is necessarily insensitive to the level of stress or strain [Guimaraes, 1992]. Essentially, this would allow a final model to be a summation of all independent contributions, vastly simplifying the problem. A diagram showing this cumulative effect is included below.

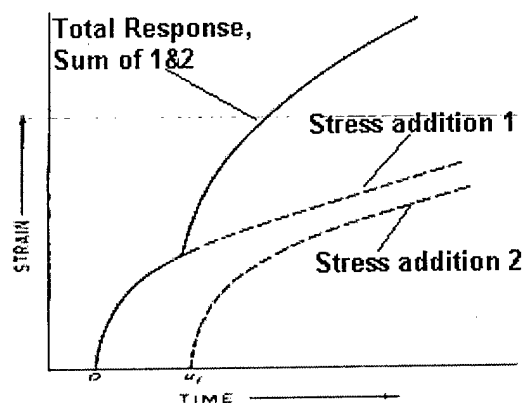


Figure 2.2: Boltzmann Superposition for Creep [Aklonis, 1983].

There has been a large body of research demonstrating that Kevlar in fact behaves as a Non-Linear Viscoelastic material as noted in the Fundamentals section. The most extensive work was performed by Wortmann and Schulz and published from 1994 to 1995. They propose a two-component model and have developed master curves. However, their work was performed on Kevlar 29, which has previously been noted to have a different and more complicated response than Kevlar 49. Wang notes non-linearity under cyclic moisture conditions and at higher initial loads, and references other investigators also [1992].

## 2.6 Humidity Variable:

Wang et. al. have done an extensive and quantitative review of the mechanosorptive behavior of Kevlar. They have reported activation energies for high, low, and cyclic humidity, and include a temperature variable with the Arrhenius equation and these activation energies. However, they do not provide information about the full spectrum of humidity. They make an

observation that the equilibrium moisture content in Kevlar fibers is only slightly affected by temperature and does not substantially influence the creep rate. This may be an important simplification.

Accelerated creep in Aramid Fibers is an established phenomenon [Habeger, 2001].

“Accelerated creep is a prime example of a transient effect. Hydrophilic materials almost always exhibit increases in creep compliance with increasing moisture content. Nonetheless, they often experience even greater creep in cyclic humidity environments...” [Habeger, 2001]

Habeger notes the importance of correct cycling times (from 10 % to 90 % RH) to induce accelerated creep, and at times over 200 minutes notes no accelerated creep [2001]. Kevlar exposed to changing environmental conditions within NASA’s applications and this investigator’s imagination will not be repeatedly cycled at frequencies higher than 200 minutes. Therefore, the cyclic effects were not studied. However, the response of Kevlar in the full range of humidity conditions should be quantified in a full investigation. This is recently motivated by rapid load loss observed in Kevlar loops in the EOS program at very low humidity, and the use of the fibers in the vacuum of space.

Because this factor is established as having some observed significance, it is important that all testing consider the relative humidity and the moisture content of the fiber. Thus, a preconditioning procedure should be used on each specimen tested to obtain uniform moisture equilibrium. Specific data on the moisture regain properties of Kevlar are reported in the following figures from DuPont’s Product Manuel [Kevlar, 2003].

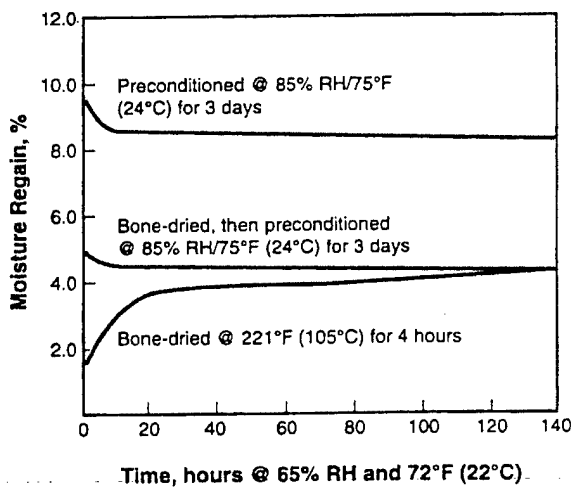


**FIGURE 2.3. Moisture Regain of KEVLAR® 2 (After Various Preconditionings).**

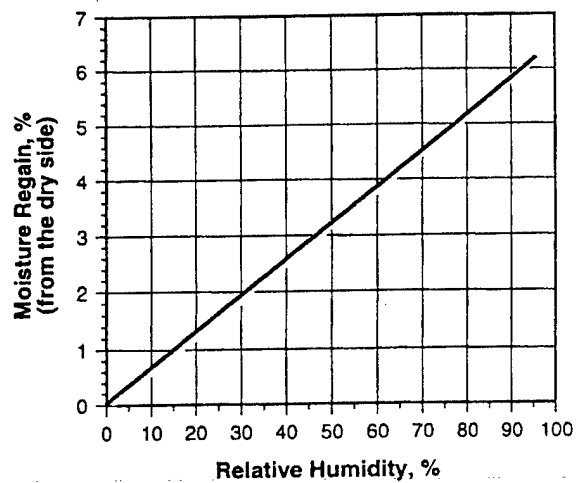


**FIGURE 2.4. Equilibrium Moisture Content of KEVLAR® 49 vs. Relative Humidity at Room Temperature.**

Figure 2.4. Moisture Properties of Kevlar Aramid Fiber [Kevlar, 2003].

Another factor that should be considered is a possible direct expansion or contraction with moisture. If a CME is significant, it needs to be included in the final model. In the same way as the CTE, this could also lead to interdependencies. An indication of such a direct response is seen in Figure 6. of Report 99-61 from NASA Goddard 541, and is included below.

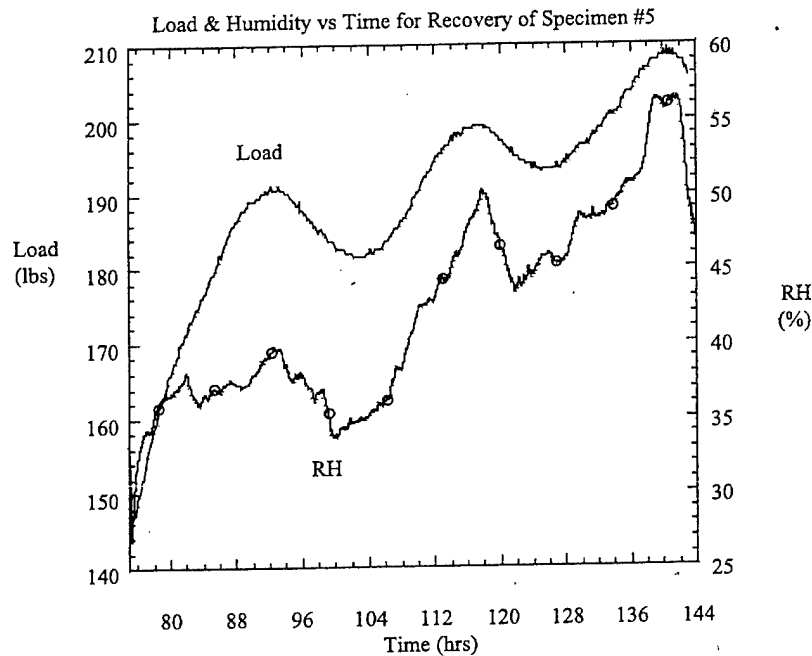


**Figure 2.5: Load and Relative Humidity Versus Time Recovery of Kevlar [NASA, Jun 1999].**

## **2.7 Pressure Variable:**

The only available information on the effects of pressure comes from Nielsen who reports pressure effects on creep and stress relaxation only at extremely high pressures (30,000 psi) where it tends to increase relaxation time [1994]. Due to the rarity of products seeing such application, this effect was not studied. However, the effects that a vacuum may have on other factors such as the rapid drying of the fiber must be accounted for.

---

## **2.8 Recovery Variable:**

Analysis of a complex loading history will necessarily need to account for the response of the fiber if the strain is removed and then reapplied. There is no evidence at all for this phenomenon as it relates to stress relaxation, but only creep. Erickson notes an immediate reduction in strain followed by further reduction in strain with time, which was linear with log time for the time frame it had been originally in creep. Afterwards, there was a departure from semi-log prediction and less recovery was seen [Erickson, 1985].

## CHAPTER 3

### RESULTS AND ANALYSIS:

#### 3.1 Specimen Buildup:

The first project undertaken was developing a suitable test specimen. The material being investigated was braided Kevlar (B49 16x1420x6 and B49 16x1420x4) as described in the Background section. Ideally, the specimen should be uniform between the grips with all fibers in the braided cord equally stressed. Conversations with Mr. Michael Viens and Mr. Dave Puckett, along with correspondence with Mr. Jerry Sterling at Wallops Space Flight, and Doug Bentley of Cortland Cable led to the development of the final test specimen buildup for the braided cord.

Eye splicing the single braid cord is the only feasible method to provide universal loading on all fibers and high strength capability. These experiments used a very simple Bury splice, and did not taper the ends of the splice or include any whipping or lock stitching, which can further increase the strength. A diagram of a Bury splice is included below.

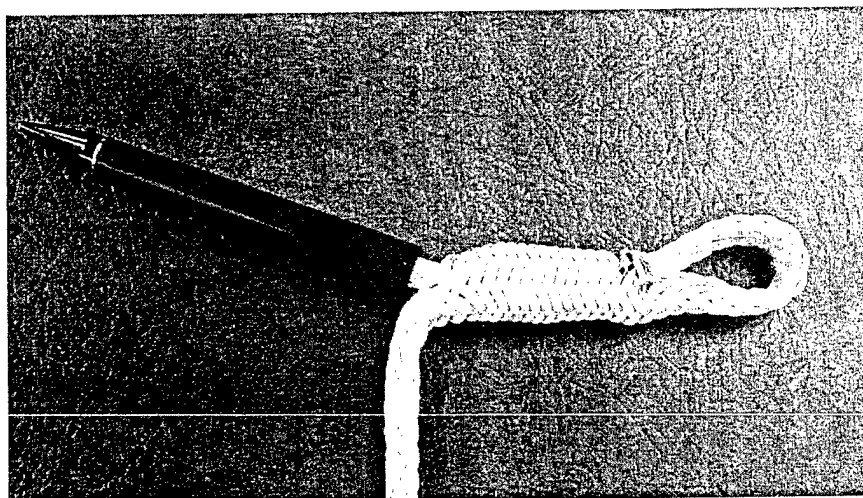


Figure 3.1: Bury Splice of Kevlar Specimen.

Each specimen is made from a 25-inch length of cord. The ends are formed into loops using Bury splices, leaving the specimen 15 inches long with 6 inches remaining in the midsection, as pictured below.

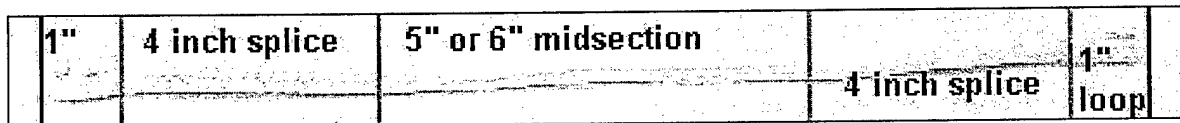


Figure 3.2: Dimensioned Picture of Test Specimen.

The dimensions were designed to give the minimum splice length without failure by pullout of the splice, coupled with the maximum length of un-spliced, uniform material in the midsection. The overall length was limited by the two-foot long relaxation cells to be used, which were themselves limited by the size of the environmental chamber and INSTRON 4400 to be used to load each cell. A four-inch splice was required to prevent failure by pullout. At least a one-inch long eye loop was necessary to fit around the pin holding the cord. For the first three test runs, the middle section was actually 6 inches long (using 26 inches of total cord), but then reduced to compensate for a change in the fixturing.

The specimens are tested at different percentages of their ultimate load. Because the literature review demonstrated that a purely theoretical calculation of ultimate load did not follow actual material values closely due to the splice and braid, further strength testing determined a baseline ultimate load. These values were intended to establish a general ultimate load to design our experiments off of, and were considered estimates only. They are not intended to be precise material properties, but instead reflect failure for specimens built and spliced in the above manner. The majority of failures occurred at the splice transition, as was expected from conversations with Cortland Cable. Tapering the end of the splice to mitigate the

stress concentrations may increase the strength. The results of these strength tests are summarized in the table below.

Table 3.1: Summary of Strength Testing.

Cordage	Failure gpd	% of 23 gpd	STDEV	Failure Mode
B49 16x1420x6	15.94	69.30	1.290	Loop base
B49 16x1420x6	16.30	70.88	Average	Splice transition
B49 16x1420x4	17.25	75.01	17.080	Splice transition
B49 16x1420x4	18.83	81.86		Splice transition
Performed on INSTRON 4485 at 0.5 in crosshead speed to specimens with twin 4 inch eye splices. 23 gpd represents literature material ultimate stress from Yang, pg 30.				

Specimens were spliced by hand for each relaxation test. Excess specimens were made and test specimens chosen at random from this pool. Some of the specimens chosen were from the outer-most layer on the spool, and some from further in. Those on the outer layers showed visible discoloration from UV exposure and aging. This is a possible source of error. Attempts to gain insight into the effect of UV exposure were unsuccessful. Other possible sources of sample error include: Non-uniform dimensions, non-uniform splice transitions, and abrasion induced upon sample loading.

There were other ideas considered and discarded as it was discovered that the most strength was achieved with splicing. This is supported by literature that indicates that in our conditions, a knot would give us 75% strength at best (bowline knot), while a proper eye-splice yields 90% of the rope strength [New England, 1999]. Tensile testing of various configurations to failure such as knotted and various length splices supported this claim. An idea of potting the ends of the cord into a hollow, threaded steel bar was abandoned due to the difficulty of potting all fibers uniformly. This potting would need to be undertaken at the same maximum load seen in relaxation testing so that additional stress concentrations would not occur. At this load, the yarns and individual fibers are so tightly packed that the adhesive has no room to occupy the

cord. Split capstan, or barrel grip methods often used for cables are unfeasible due to the diameter and construction of the cord, as are the simple clamp methods used for fibers.

### 3.2 Test Setup:

The design of the test setup required the control all of the variables expected to affect Kevlar, the ability to run as many concurrent specimens as possible, and autonomous operation for at least two weeks at a time. The test fixtures used will be referred to as relaxation cells, or cells. The setup of the relaxation cell is pictured below.

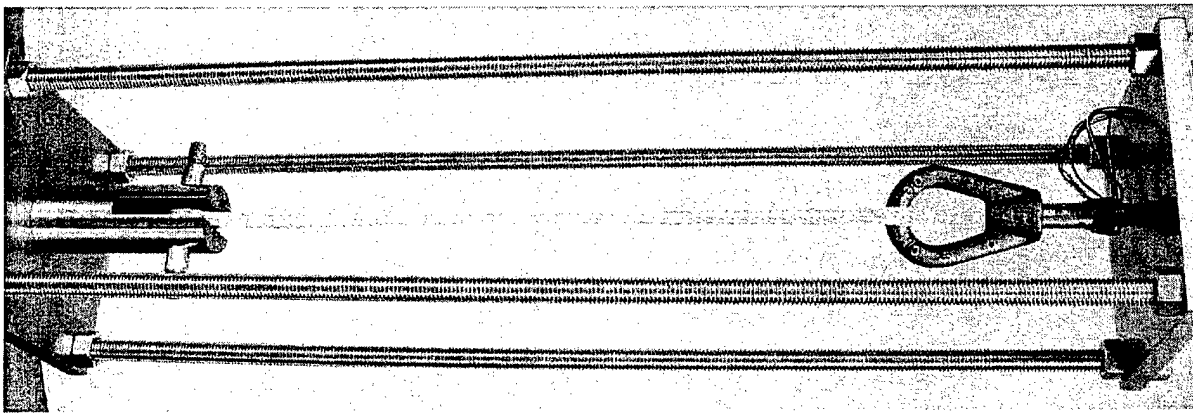


Figure 3.3: Relaxation Cell Depiction.

These fixtures were previously used to measure load relaxation of EOS AURA, and AQUA solar array restraints. As the EOS application uses the Kevlar in a loop, some fixture modification was required. The cells are stainless steel, consisting of four,  $\frac{1}{2}$ "-13 threaded bars two feet long, with a  $\frac{1}{2}$ " stainless steel plate bolted to each end. Through a center hole in each plate, a yoke is attached. The bottom yoke is fixed, and the top slides freely through the hole until stopped by a nut on the threaded bar holding the yoke. Half-inch pins through the eye splice grip the specimen at the bottom, while the top yoke is a cast eye nut, pictured below, and requires the cord to be spliced around it. Each cast eye-bolt was polished by hand with the assistance of Mr. Dewey Dove to prevent abrasion of the cords.

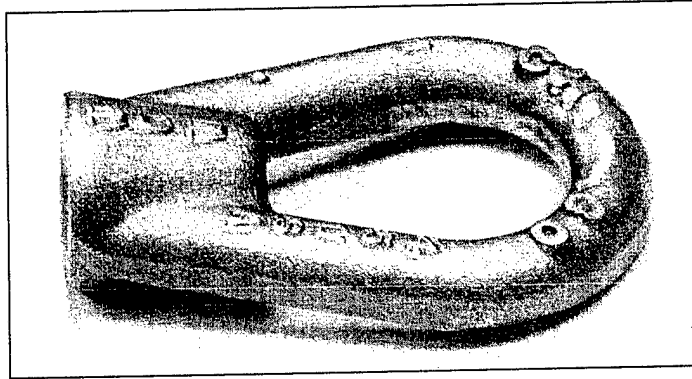


Figure 3.4: Cast Eye Bolts.

The steel tensioning bar was fitted with strain gages and calibrated for load. A Micro Measurements EA-06-125AC-350 gage was attached to four sides of the smooth steel bar (every 90 degrees) and aligned by eyesight to be along the tensile axis. The strain of all four was averaged to report a tensile strain, and then converted to load with an experimental calibration constant. For the first three test runs, only two of the four gages were in place, the second pair being added at this time to further reduce possible error from bending.

During initial calibration of the system, a dummy specimen was loaded into each cell and then each cell loaded into an INSTRON 4485 mechanical testing machine. They were tensioned at 0.5-in/min-crosshead speed up to 80% of the load seen in the strength tests. This data was then plotted against the average of the two strain gages. The resulting curve was almost perfectly linear. However, it was necessary to repeat this loading sequence three to four times to obtain consistency in the resulting slope constant. This has been noted by Mr. Puckett before and may be a settling of the strain gage. In the end, the calibration constant was set during the actual specimen loading process by base-lining at zero load, and setting the calibration constant to be accurate at 1000 lbs. Variations due to fixture orientation and the thermal environment are suspected to have caused the calibration constant to vary between tests.

In order to precisely control humidity and temperature, which have been shown to have direct effects on the tension of Kevlar, a sealed Plexiglas test chamber was employed. A simple incandescent light bulb with a temperature controller was used as a heat source, which was able to consistently hold the test chamber within  $2/10^{\text{th}}$  of a degree C for temperatures slightly above room temperature. A humidifier, de-humidifier, and controller held the chamber within 1% relative humidity while the chamber was closed. A list of the specific equipment can be found as Appendix D. A photograph of the environmental chamber with a relaxation test running is shown below.

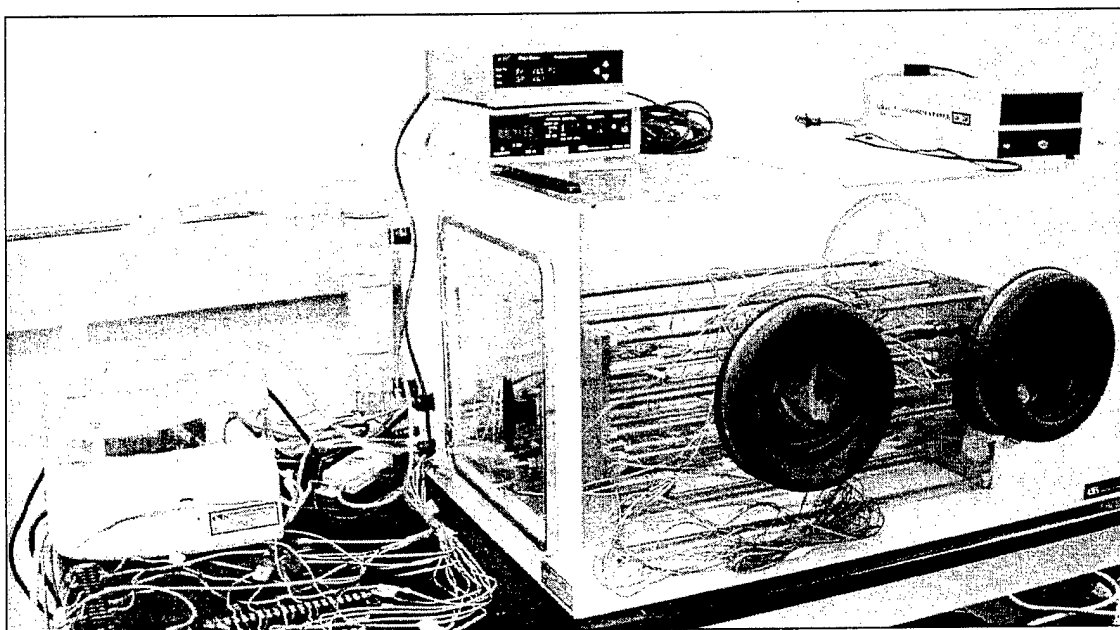


Figure 3.5: Environmental Chamber and Kevlar Cells.

Testing by Mr. Puckett previously demonstrated that temperature in the chamber was constant throughout, and a fan continuously circulated interior air to maintain uniformity of both humidity and temperature. Other than temporary heat failure (bulb burnout) or a block of the humidifier, the chamber showed exemplary performance. It is not expected to have been a source of error.

### 3.3 Preconditioning/Loading:

Some specimens were preconditioned to achieve uniform moisture content prior to testing in an INSTRON test oven at specified temperatures and times prior to testing. The specific treatment given to each specimen is outlined in Table 2. Preloading/relaxation is done within the test-cells on an INSTRON 4400R as pictured below. The primary phase (or preconditioning) of relaxation refers to the relaxation observed after initial loading. For this test, a relaxation cell is placed into the machine, and the Kevlar load path is loaded to the preconditioning value reported in Table 2, according to the load cell of the machine. During this loading phase, the strain gages of the relaxation cell are calibrated. Then, data is taken from the strain gages for approximately 30 minutes while the crosshead of the INSTRON is held constant. The range of data begins at the stop of the machine crosshead at the preconditioning load, and ends when the crosshead moves again to make up the load lost due to this initial relaxation.

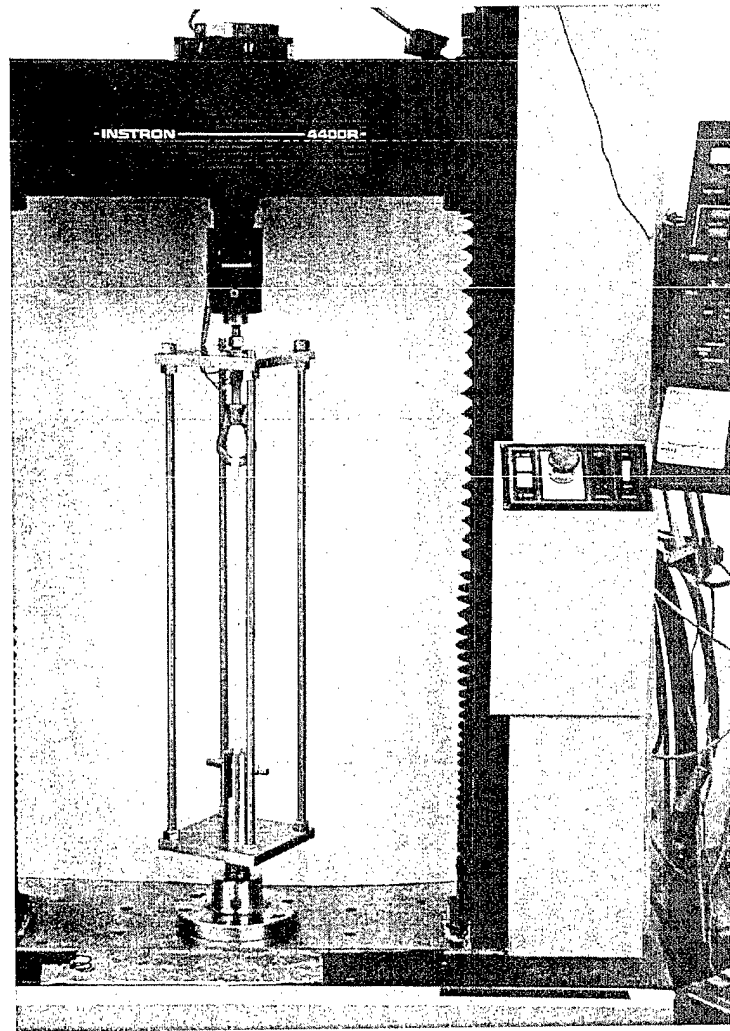


Figure 3.6: Preconditioning and Loading in the INSTRON.

Each specimen was loaded individually in its cell in the INSTRON machine, and allowed to relax for a pre-determined time (generally 30 minutes). It was then re-tensioned to the final test load, and the nut on the cell tightened to transfer the load completely into the cell. The relaxation cell was then removed from the INSTRON and placed into the environmental chamber, and the next cell was loaded. Once all cells were in place, the environmental chamber was sealed and conditions held constant. The specific conditions for each data run are reported below in Table 2.

Table 3.2: Testing Conditions for Kevlar.

Kevlar Testing Conditions											
	Date	Product	Setup	Pretensioning		Preconditioning		Temp	Humidity	Initial Load	Total Time
				load (lbs)	time (min)	temp (K)	time (hr)	(K)	(%)	(lbs)	(d)
1.1	22-Oct	K49-6	2gage yk	2250	30	333	20	300	60	2250	19.1
1.2	22-Oct	K49-6	2gage yk	2250	30	333	20	300	60	2250	19.1
1.3	22-Oct	K49-6	2gage yk	2250	30	333	20	300	60	2250	19.1
1.4	22-Oct	K49-4	2gage yk	2250	35	333	20	300	60	2250	19.1
1.5	22-Oct	K49-4	2gage yk	2250	30	333	20	300	60	2250	19.1
2.1	10-Nov	K49-6	2gage yk	2250	30	333	20	300	60	2250	22.8
2.2	10-Nov	K49-6	2gage yk	2250	30	333	20	300	60	2250	22.8
2.3	10-Nov	K49-6	2gage yk	2250	30	333	20	300	60	2250	22.8
2.4	10-Nov	K49-4	2gage yk	2250	30	333	20	300	60	2250	22.8
2.5	10-Nov	K49-4	2gage yk	2250	30	333	20	300	60	2250	22.8
3.1	3-Dec	K49-6	2gage yk	2250	26	333	20	300	60	2250	7.0
3.2	3-Dec	K49-6	2gage yk	2250	25	333	20	300	60	2250	7.0
3.3	3-Dec	K49-6	2gage yk	2250	25	333	20	300	60	2250	7.0
3.4	3-Dec	K49-4	2gage yk	2250	75	333	20	300	60	2250	7.0
3.5	3-Dec	K49-4	2gage yk	2250	25	333	20	300	60	2250	7.0
4.1	19-Dec	K49-6	4gage eye	2250	30			300	60	2250	17.3
4.2	19-Dec	K49-6	4gage eye	2250	30			300	60	2250	17.3
4.3	19-Dec	K49-6	4gage eye	2250	30			300	60	2250	17.3
4.4	19-Dec	K49-4	4gage eye	2250	30			300	60	2250	17.3
4.5	19-Dec	K49-4	4gage eye	2250	30			300	60	2250	17.3
5.1	12-Jan	K49-6	4gage eye	1500	20			300	60	1500	14.8
5.2	12-Jan	K49-6	4gage eye	1500	20			300	60	1500	14.8
5.3	12-Jan	K49-6	4gage eye	1500	35			300	60	1500	14.8
5.4	12-Jan	K49-4	4gage eye	1500	20			300	60	1500	14.8
5.5	12-Jan	K49-4	4gage eye	1500	20			300	60	1500	14.8
6.1	28-Jan	K49-6	4gage eye	2250	30	333	20	300	60	2250	63.3
6.2	28-Jan	K49-6	4gage eye	2250	30	333	20	300	60	2250	63.3
6.3	28-Jan	K49-6	4gage eye	2250	30	333	20	300	60	2250	63.3
6.4	28-Jan	K49-4	4gage eye	2250	30	333	20	300	60	2250	63.3
6.5	28-Jan	K49-4	4gage eye	2250	30	333	20	300	60	2250	63.3

Kevlar reacts relatively slowly to temperature changes, and also absorbs moisture at a slow rate, both of which affect its mechanical properties. There is a brief period during the move from the drying oven to the environmental chamber where the temperature and humidity of the test specimens are not controlled. Preconditioning was skipped for some test runs, as noted in Table 2. The results were not consistent enough to determine any results of this change.

### **3.4 Data Acquisition:**

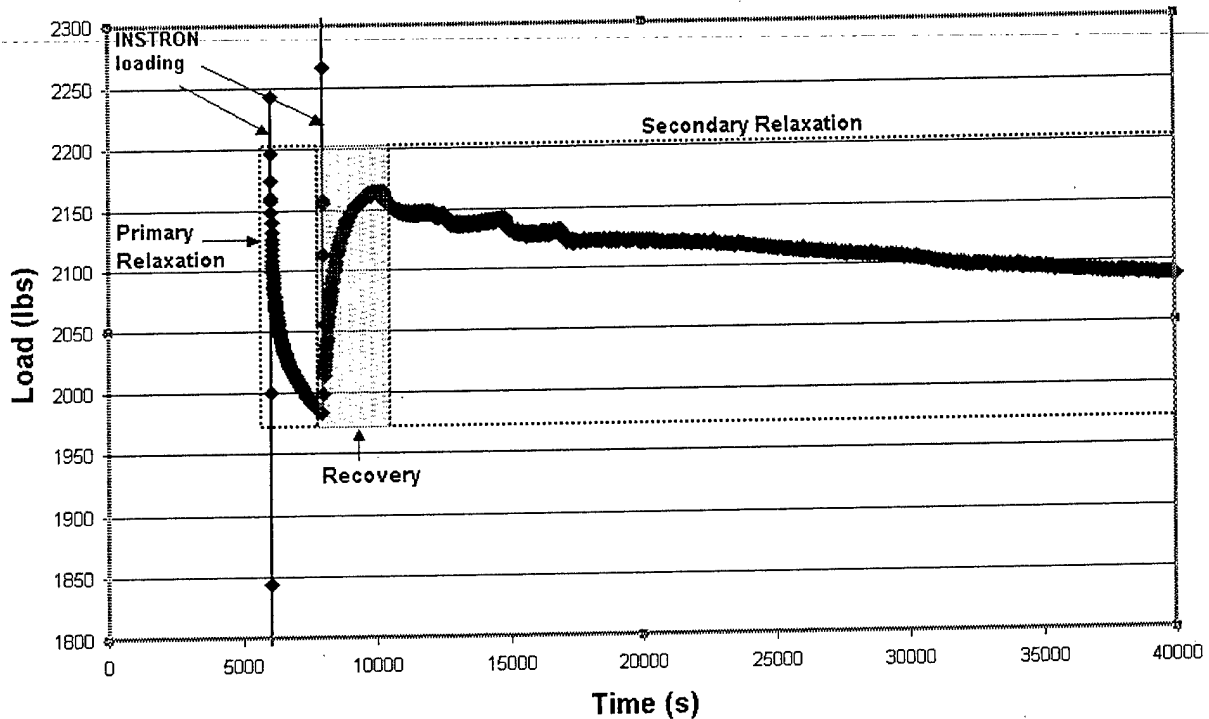
A Macintosh computer running LabVIEW 5.0.1 recorded the data through a Hewlett Packard Data Acquisition/Control Unit. The strain gages were excited at 3V. The data output from four strain gages was averaged for each unit and multiplied by a calibration factor. The manufacturer's suggested gage factor was used for each gage, and then the calibration factor added to the average of the four gages to report load in lbs. This was recorded along with room temperature, chamber temperature, chamber relative humidity, and a time stamp. Initially these were recorded approximately 10 seconds apart. After at least one hour of relaxation, the time between data points was increased, up to 600 seconds. The lead wires from the chamber to the environmental chamber to the data acquisition unit are 6 ft long, and induce slight fluctuations as room temperature changes.

### **3.5 Data Analysis:**

The data was analyzed primarily in Microsoft Excel. The raw data file was imported into Excel, and then manipulated to normalize the start time (to 1 second = end of loading sequence/start of relaxation) since each cell had to be loaded sequentially. Then, separate plots were generated for the primary relaxation, the overall secondary relaxation period, and a plot showing the pure relaxation behavior which began after the recovery period in the secondary plot. This recovery period represents the first 4000 seconds (about 1 hour) after the cell has been reloaded following initial relaxation. During this time, there is load increase due to temperature and humidity changes from the ambient environment to the test chamber, and a suspected memory recovery due to previous tensioning such as noted for creep by Erickson. A best-fit logarithmic form was used in Microsoft Excel to fit the data and obtain the slope constants.

A graph showing these periods as load vs. time for a typical test run is pictured below. Note that after the second INSTRON loading, the load immediately drops again to below 2010 lbs. This is typical of load lost during the tightening of the nut that transferred the load to the relaxation cell.

### Summary of Testing cycle



*Note that the second spike for "Instron Loading" also includes a decrease in load as load was transferred to the frame. In this case, the fixture lost almost 250 lbs during tightening of the nut to transfer the load, and the recovery period started at around 2010 lbs.*

Figure 3.7: Summary of Testing Cycle.

This relaxation plot was fitted for each fixture by a best-fit log equation. The slope in units of lbs/log(t) was reported to a summary sheet, as well as the "R squared" value. A slope constant was also reported for the primary relaxation. Finally, a plot of the environmental variables and all the fixtures was included. Each of these environmental variables was

amplified to allow an easy graphic search for the potential environmental explanation of inconsistencies in the relaxation data.

All average slope numbers and comparisons are made with "valid" slope constants. For a slope constant to be considered valid, it was required to meet the following requirements.

- 1) The value must be accompanied by an  $R^2$  value of at least 0.96. This number is necessarily low in order to account for scatter in the data due to unintentional environmental changes, and unresolved causes. It is high enough to require a consistent slope trend.
- 2) The value must have been obtained over the entire data set from the end of recovery to the termination of the test.
- 3) Exception to the above includes that any small periods of data representing a failure of environmental equipment may be deleted. Therefore, data during a period of temperature drop due to the heat lamp failing can be eliminated and a valid slope obtained if the lamp was quickly replaced, or if failure occurred at the end of the test.

### 3.6 Results:

A complete collection of all the test graphs can be found in Appendix F. The graph below represents a compilation of all the valid slope constants, along with the average values and their standard deviation. The large point to the right of each cloud of data points represents their average value, and the error bar represents their standard deviation. A best-fit logarithmic form was used in Microsoft Excel to fit the data and obtain these slope constants. The values for these points and for the discarded invalid points are reported on the next page.

#### Summary and Comparison of Valid Slope Constants

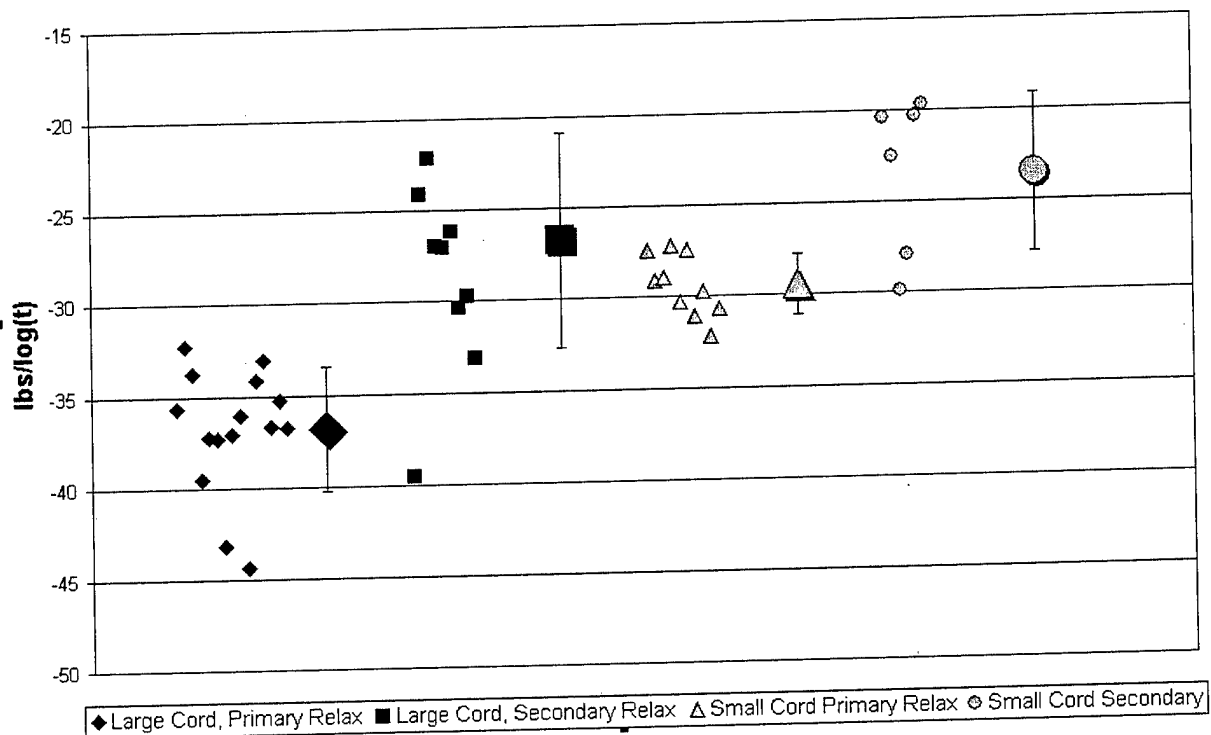


Figure 3.8: Summary and Comparison of Valid Slope Constants.

The following table is a summary of all the slopes obtained in testing.

Table 3.3: Summary of all Slope Constants.

Summary and Comparison of Slope Constants									
Large Diameter Cord					Small Diameter Cord				
	Primary		Secondary			Primary		Secondary	
	lbs/log(t)	R squared	lbs/log(t)	R squared		lbs/log(t)	R squared	lbs/log(t)	R squared
Test 1.1	-35.664	0.9975	<u>-12.217</u>	<u>0.9507</u>	Test 1.4	-27.459	0.9968	-20.398	0.9791
Test 1.2	-32.236	0.9959	-39.541	0.9916	Test 1.5	-29.112	0.9951	<u>8.2332</u>	<u>0.4045</u>
Test 1.3	-33.761	0.9957	-24.08	0.9783	Test 2.4	-28.951	0.9942	-22.548	0.9699
Test 2.1	-39.551	0.9969	-22.089	0.98	Test 2.5	-27.194	0.995	<u>-10.971</u>	<u>0.6783</u>
Test 2.2	-37.287	0.9958	-26.972	0.9913	Test 3.4	-30.269	0.9962	-29.91	0.9873
Test 2.3	-37.359	0.9946	-27.001	0.9912	Test 3.5	-27.43	0.9932	-27.875	0.9813
Test 3.1	-43.21	0.9864	-26.137	0.9913	Test 4.4	-31.067	0.9968	<u>48.342</u>	<u>0.7752</u>
Test 3.2	-37.111	0.9931	-30.397	0.9922	Test 4.5	-29.743	0.9811	-20.273	0.9809
Test 3.3	-36.088	0.9945	-29.697	0.9917	Test 5.4	<u>-24.593</u>	<u>0.9942</u>	<u>-1.3807</u>	<u>0.0447</u>
Test 4.1	-44.394	0.9866	-33.15	0.9975	Test 5.5	<u>-22.031</u>	<u>0.9916</u>	<u>-14.001</u>	<u>0.8658</u>
Test 4.2	-34.152	0.9934	<u>-19.148</u>	<u>0.9234</u>	Test 6.4	-32.147	0.9989	<u>-0.9075</u>	<u>0.7082</u>
Test 4.3	-33.082	0.9753	<u>-7.5178</u>	<u>0.5183</u>	Test 6.5	-30.657	0.9979	-19.711	0.9685
Test 5.1	<u>-37.202</u>	<u>0.9689</u>	<u>-26.232</u>	<u>0.9796</u>	Notes <i>Numbers underlined and in italics are invalid</i>  Test 5 data is invalid due to a humidity issue that negated the first day of data collection				
Test 5.2	<u>-30.797</u>	<u>0.974</u>	<u>-18.051</u>	<u>0.9572</u>					
Test 5.3	<u>-29.472</u>	<u>0.9897</u>	<u>-15.114</u>	<u>0.9464</u>					
Test 6.1	-36.717	0.9981	-23.198	0.9937					
Test 6.2	-35.254	0.9921	-20.271	0.982					
Test 6.3	-36.752	0.9983	-18.357	0.9717					

The graph below shows example test runs that generated invalid slope constants. This graph shows 5 specimens. The three thick lines represent large diameter cord, and the small lines represent smaller diameter cord. Each began with the same approximate load, so the small cords have a higher stress. Pretreatment and test conditions are the same for all.

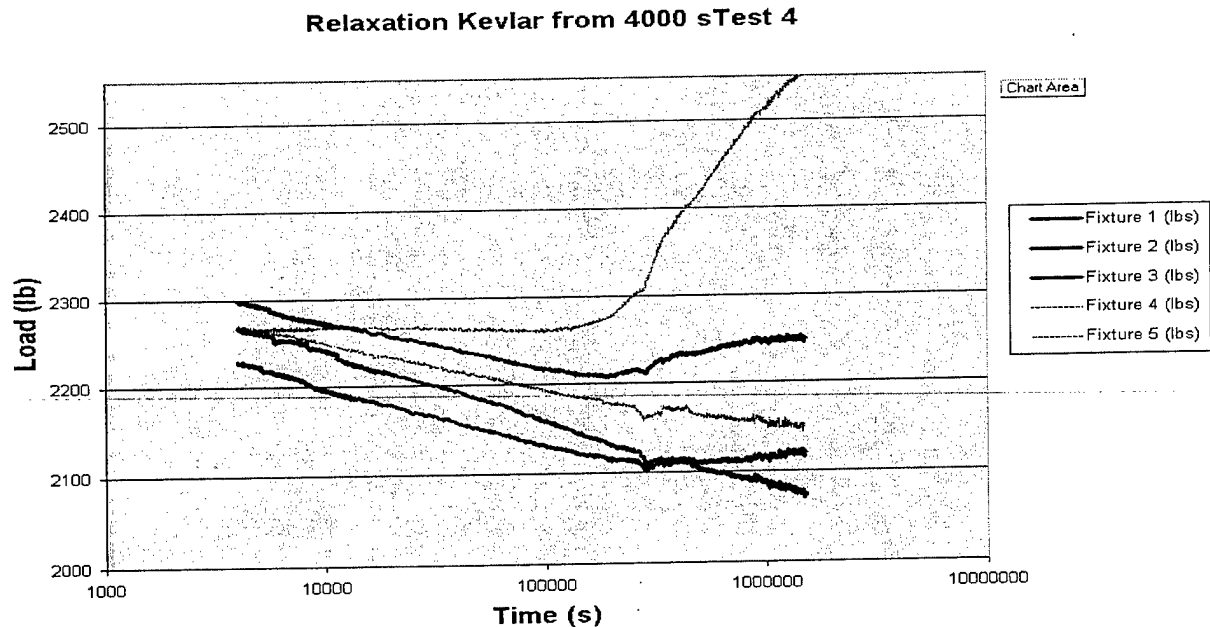


Figure 3.9: Display of Erratic Kevlar Behavior.

The table below shows the average values for both primary and secondary relaxation for the two cord sizes tested, representing only valid slopes. Since all valid slopes were obtained using the same load (2250 lbs), and because both cords were of the same construction, the difference between the small and large diameter cord can also be stated as medium vs. high stress. Bold numbers represent the literature values reported for comparison.

Table 4: Average Slope Constants.

Large Diameter Cord			
Primary		Secondary	
lbs/log(t)	STDEV	lbs/log(t)	STDEV
-36.841	3.40214	-26.7408	5.88475
%/log(t)	Blades	%/log(t)	Blades
-0.0164	<b>-0.016</b>	-0.01188	<b>-0.0096</b>

Small Diameter Cord			
Primary		Secondary	
lbs/log(t)	STDEV	lbs/log(t)	STDEV
-29.403	1.685791	-23.453	4.37067
%/log(t)	Blades	%/log(t)	Blades
-0.0131	<b>-0.016</b>	-0.0104	<b>-0.0096</b>

### Overall Valid Results

	lbs/log(t)	%/log(t)
Primary Relax	-33.87	-0.0151
Standard Deviation	4.65	0.0021
Secondary Relax	-24.65	-0.0110
Standard Deviation	6.17	0.0027

## CHAPTER 4

### CONCLUSIONS

#### 4.1 Primary Relaxation

The results of the primary relaxation are demonstrative of three important findings. The first is that the **initial relaxation phase is generally log-linear**. The equation below describes the response, where stress and load are considered interchangeable since the area remains constant. 23 of 30 curves demonstrated an  $R^2$  fit of the log-linear model above 0.99, and the worst fit was 0.97.

$$\sigma = \sigma_1 + \beta \text{Log}(t)$$

The second finding of this phase of testing is an average **relaxation rate ( $\beta$ ) of -0.0151 %/log(t)** with a standard deviation of  $\pm 0.0021$ . The only other reported value for Kevlar relaxation (Blades, 0.016 %/log(t)) falls well within this range.

The third finding reinforces Guimaraes' rope study in showing that the secondary relaxation phase is a smaller percentage of this original phase. This study found the preconditioning relaxation phase to represent a **41 % higher relaxation rate** than the secondary phase.

These relaxation values are averages, and do not take into account any effects of material dimensions, environmental conditions, load values. The test time was about 30 minutes each. They define approximate relaxation for Kevlar 49 braided cord tested in room temperature and humidity ranges with most loads over 50% of ultimate strength.

#### 4.2 Secondary Relaxation

In applications where relaxation is of interest, Kevlar will most likely experience a re-tensioning, making this variable of key interest. This variable was expected to be the most

consistent since effects of the weave, twist, and braid of the cord would be minimized after initial tensioning. The testing periods for this secondary phase were usually 2 orders of magnitude longer than the primary phase (2 weeks long). Kevlar's secondary relaxation generally fits a **log-linear relaxation** model as expected from the literature. Proof for this comes from the high R squared values seen on most of the tests when fitted to a logarithmic curve.

Kevlar exhibits **secondary load relaxation at a rate ( $\beta$ ) of approximately  $-0.0110 \pm .0027 \text{ lbs/log(t)}$** . This represents the culmination of 18 valid slope data points. It is an average of the two braided cords, with error defined as the standard deviation across the 18 points. This is for loading at approximately 60-80% of the ultimate strength, at 26.7 C and 60% relative humidity. With the highly erratic data points disregarded (those which markedly did not fit a semi-log plot according to their "R squared" value and were classified invalid) this is at least a reasonable estimate of load loss that can be expected in Kevlar braided cord. Also, as described in the primary relaxation section, the secondary rate of relaxation shows a 40% reduction in slope compared to primary relaxation. This change is consistent with both the behavior seen in parallel lay rope and previous fiber studies.

The data invariably experienced a **short recovery period after re-tensioning** and transferring the load to the relaxation cell. Recovery was also noted by Erickson and Guimaraes for creep. The average time in these tests defined as the time to semi-log relaxation was 4000 s (about 1 h) recovery. It must be noted that this cannot be necessarily correlated with Kevlar, or expected to occur as observed in all applications. The recovery period also coincides with time that the fixture and sample enter the chamber and reach equilibrium for both a slightly increased temperature, and humidity. It is entirely possible that this is purely an environmental

effect. Also, the time length cannot necessarily be inferred for all other loading conditions, and it is a subjective determination of the initiation of log-linear relaxation.

### 4.3 Sources of Error

We experienced several anomalies that bear discussion. Especially noteworthy were several instances of a positive slope. This was observed once in almost every test run after an initial period of relaxation, and generally occurred in fixture 4 or 5 with the small diameter (x4) cord and higher % of ultimate load. The curves in Figure 3.9 demonstrated some of these erratic slopes. Investigations into the cause of this anomaly yielded no definitive answers.

First, a test was run using a steel bar in place of the Kevlar straps. These tests showed no increase in load over time. Temperature and humidity have been demonstrated to be uniform throughout the chamber. There is a possibility of bending or torsion in the load cells, which motivated the move to averaging 4 strain gages for load and the use of an eye-bolt.

The actual increase in load over time for Kevlar should not be possible, and seemed to be a repeated problem in fixture #4. The mechanism that might cause this anomaly is not understood, especially since the load appeared normal through initialization. Possible causes include physical changes (bending, slipping, twisting) over time in the cell due to changing tension of the Kevlar, or a slightly erratic strain gage. However, further testing is required to rule out some kind of memory effect in the Kevlar material itself.

A question was raised as to whether the stored cordage had lost strength or possessed different properties where it had been exposed to UV radiation in the room, and been slightly discolored to a deeper gold compared to the rest of the spool. To discount this possibility, a UV lamp was used to bake several specimens directly for several hours, which were then loaded into an experiment. No observable change in behavior was seen.

Attempts to model the effects of temperature on the Kevlar became difficult very quickly. The cordage does not respond to temperature immediately. However, the steel fixturing responds very quickly, and in an opposite manner. Steel has a positive CTE, while Kevlar has a negative CTE. Therefore, any temperature fluctuations become very difficult to precisely model. It became apparent that studying the effects of Kevlar's CTE, or change in relaxation behavior from a temperature change might be impossible with this test setup if the steel induced or removed load from the Kevlar. Future investigations would need to develop fixturing with a negligible CTE that would not induce any effect on the Kevlar during a temperature flux. Also, Kevlar is slow to respond to temperature changes. Therefore, when attempting to eliminate the effects of minor temperature fluctuations, or loss of chamber heating, a ramp time must be included in the model.

The direct effect of chamber temperature on the test frame and specimen as described above can be easily recognized in Figure 5.1 below. The lead wires of about 6 feet, which led from the environmental chamber to the computer, are suspected to be the cause of the small correlation of load in lbs to the room temperature. This phenomena can be observed in Figure 5.1 during the first part of the curve where chamber temperature is constant.

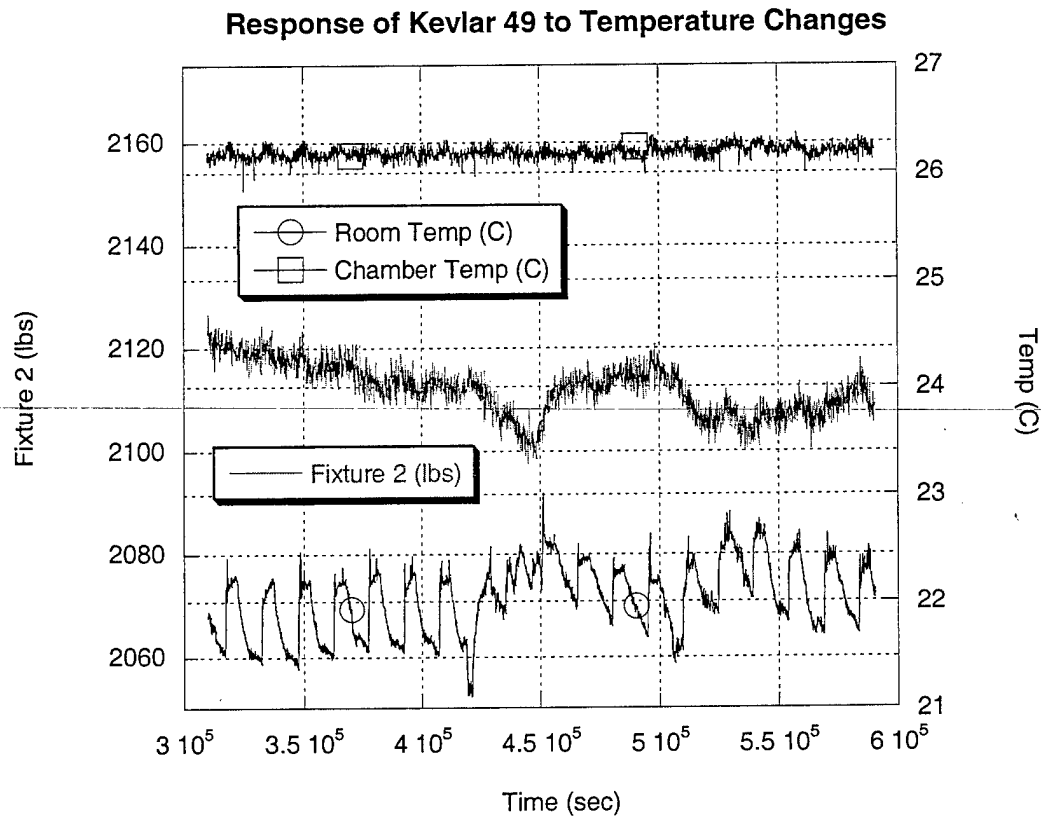


Figure 4.1: Response of Kevlar 49 to Temperature Changes.

The effects of moisture are easier to study with this test setup since steel has no CME. However, a major difficulty is encountered in separating the effects of humidity changes from the normal relaxation in Kevlar (this is also an issue with temperature). First, it is significant that Kevlar is known to absorb moisture very slowly, over about 1-2 days (refer to Figure 2.4). Second, due to the erratic nature of results seen, defining what should be the relaxation behavior at time (t) to be subtracted from the cumulative effects of moisture and normal relaxation becomes very difficult.

#### 4.4 Summary

The literature review shows a scatter in both the shape and quantification of creep and relaxation models. Testing for this report confirmed the popular consensus that a log-linear relaxation model applies well. Quantitative slope constants showed a high degree of variability,

as did those reported in the literature. No specific slope constant should ever be assumed to be a good prediction value.

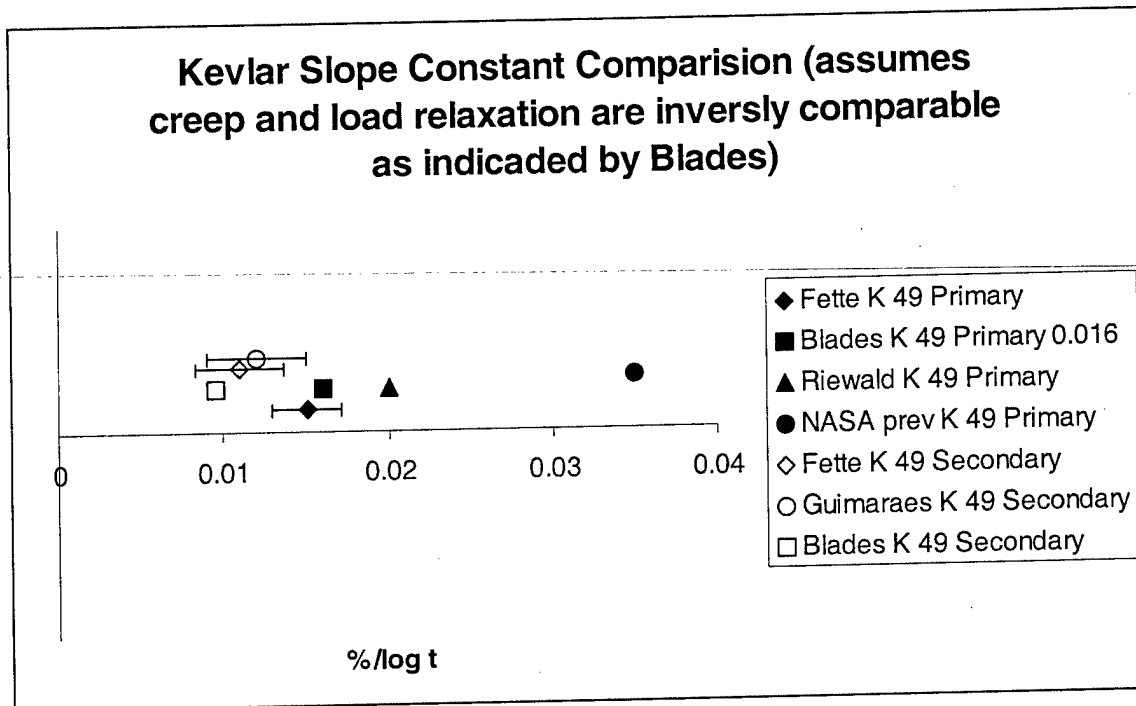


Figure 4.2: Slope Constant Comparison.

Attempts to predict the behavior of Kevlar 49 should include the use a factor of safety appropriate to the degree of variation and erratic behavior observed in predictive models. When attempting to test the material for a specific application, one should expect a high degree of scatter in the data, and conduct extensive testing to determine the full range of possible responses.

## CHAPTER 5

### FUTURE DIRECTION

Experimentation and attempts to precisely model the relaxation response of Kevlar both at NASA and in the literature have been fraught with inconsistency. The inability to satisfactorily resolve this problem through this study on Kevlar braided cord after several months of experimentation motivates the search for a replacement material which can be modeled and predicted for use in future engineering applications here at NASA, and in similar applications elsewhere. As a continuation of this work, further experimentation will begin on other new fibers and fiber combinations. Candidates include many new, high performance materials such as: High Modulus PolyEthylene (Spectra), Liquid Crystalline aromatic Polyester (Vectran), other Aramids such as Twaron and Technora, Poly [p-phenylene-2, 6-benzobisoxazole]( PBO, Zylon), and combinations of the above which may combine desirable properties. Some issues still must be resolved with the test setup for a full study including methods to analyze temperature changes during relaxation. In this case, the fixturing must have a measurable response to temperature change that translates little or no load change into the test specimen. This may be resolved through changing the material of the relaxation cells, or perhaps careful modeling of their behavior if the actual induced load change is considered negligible to the material behavior. Also, further investigation needs to be made into the initial response of the material without the complications caused by the transfer to the environmental chamber with different temperature and humidity than the room. This delta masked initial results in testing.

Russell Benjamin Fette  
2LT USAF AFIT/CIGG



U.S. AIR FORCE

## REFERENCES

- Aklonis, J. J., MacKnight, W. J. Introduction to Polymer Viscoelasticity. 2<sup>nd</sup> ed. John Wiley & Sons. 1983.
- Askeland, Donald R. The Science and Engineering of Materials. 3<sup>rd</sup> Ed. PWS Publishing Company, Boston. 1994.
- Allen, S.R. and Roche, E.J. *Polymer* 1989, Vol 30, June, conference issue
- Bently, Doug. Phone Interview. Cortland Cable. 27 Aug 2003.
- Boone, J.D. "Fatigue and Strain Characteristics of "Kevlar" Yarn and Cord under Constant Stress." American Institute of Aeronautics and Astronautics, Inc. 1975. AIAA Paper No. 75-1363.
- Brown, Roger. Ed. Handbook of Polymer Testing. Marcel Dekker Inc. New York NY. 1999.
- Bunsell, A.R. *Journal of Material Science* 10. 1975 (1300-1308)
- Cortland Cable Website, accessed 2 Oct 2003,  
<http://www.cortlandcable.com/cortlandcable/?width=1020>.
- Coskren, R.J. and Abbott, N.J. "Kevlar 29 Parachute Fabrics." American Institute of Aeronautics and Astronautics, Inc. 1975. AIAA Paper No. 75-1360.
- Dictionary.com. <http://dictionary.reference.com/search?q=denier>, Source: *The American Heritage® Dictionary of the English Language, Fourth Edition*  
Copyright © 2000 by Houghton Mifflin Company.
- Dowling, Norman E. Mechanical Behavior of Materials. 2<sup>nd</sup> ed. Prentice Hall, New Jersey. 1999.
- Duband, L. , Hui, L. and Lange, A. *Cryogenics* 1993. Vol 33, No. 6, 643-647.
- Elias, J.M., and Waugh C.E. Kevlar-Thermophysical Properties. AIAA 81-1104, 1981.
- Erickson, R.H. "The Influence of Strain Rate on the Quasi-Static Tensile Strength of Kevlar 29 Narrow Fabrics." American Institute of Aeronautics and Astronautics, Inc. 1981. AIAA Paper No. 81-1943.
- Erickson, R.H. *Polymer*. 26 733 (May 1985).
- Ferry, John D. Viscoelastic Properties of Polymers. 3<sup>rd</sup> ed. John Wiley & Sons. 1980.

Guimaraes, G.B. and Burgoyne, C.J. "*Creep Behavior of a parallel-lay aramid rope.*" Journal of Materials Science, Vol 27 1992. 2473-2849.

Habeger, C.C., Coffin, D.W., Hojjatie, B. Journal of Polymer Science: Part B: Polymer Physics, Volume 39. 2048-2062, 2001.

Kevlar Aramid Fiber Technical Guide,. Dupont Corporation. Received on 21 Aug. 2003 by e-mail.

Kunugi, T., Watanabe, H., and Hashimoto, M. *Journal of Applied Polymer Science*, Vol 24, 1039-1051. 1979.

---

Lafitte, M.H. and Bunsell, A.R. *Polymer Engineering and Science*. Vol 25, No 3. Feb, 1985.

Liquid Crystalline Polymers. The National Academy of Sciences.  
<http://www.nap.edu/openbook/0309042313/html/49.html> 1990. 2000 the National Academy of Sciences.

Petrina, P. and Phoenix, S.L. "Synthetic Ropes Subjected to Tension and Trolley Loads." 1997 IEE.

Mark, James E. ed. Physical Properties of Polymers Handbook. American Institute of Physics Press, Woodbury NY. 1996.

Matsuoka, Shiro, ed., Relaxation Phenomena in Polymers. Hanser Publishers. 1992.

Montoya, Alex, Informal interview 6 Oct 2003.

NASA Internal Report, Mr. Viens "Load Relaxation Characteristics of HST/NICMOS/Cryocooler Kevlar Straps" May 4, 1998.

... "Load Relaxation of MAP Kevlar Cord as a Function of Thermal Environment" April 15 1999.

... "Kevlar Load Relaxation Testing" Report ID 99-57, May 20, 1999.

... "Kevlar Load Relaxation Testing" Report ID 99-61, June 1, 1999.

... "Load Relaxation of MAP Kevlar Cord as a Function of Length" Sept 20, 1999.

... "Relaxation Behavior of Kevlar Cord used on the MAP Solar Array" Jan 19, 2000.

NASA Internal Report, Mr. Viens and Mr. Puckett "Thermal Knife Cut Testing of Kevlar Cord" April 25, 2000.

... "Strength Testing of Kevlar Cord used in the EOS Solar Array Deployment Mechanism"  
August 31, 2000.

NASA Internal Report, Marjorie Sovinski, on CTE of Kevlar, April 11, 2003.

New England Rope Website, accessed April 2003. <http://www.neropes.com>. 1999.

Nielsen, Lawrence E. w/ Landel, Robert F. Mechanical Properties of Polymers and Composites. 2<sup>nd</sup> ed. Marcel Dekker, Inc. 1994.

parachute cord comparison. Excerpt from web page –  
<<http://highenergysports.com/articles/winginspect.htm>.

Riewald, Paul. G. "Kevlar Aramid Fibers, Properties and Industrial Applications." Advanced Textile Materials Conference, April 5-6, 1988.

Rogozinsky, A.K. and Bazhenov, S.L. Polymer Vol 32, #7, 1992 1391-1398.

Ryan, Richard J. "High Modulus Rope Designs". Puget Sound Rope Corp. Oceans '99, Vol 2, Sept 1999. 698-701.

Schmitz, John V. ed. Testing of Polymers. Vol.1. Interscience Publishers of John Wiley & Sons, Inc. 1995.

Schoppee, M.M. and Skelton, J. Journal of Applied Polymer Science:Applied Polymer Symposium 47, 301-322 (1991).

Wang, John Z. Dillard, D.A. Ward, T.C. Journal of Polymer Science: Part B: Polymer Physics, Volume 30. 1391-1400, 1992.

Wortmann, F.J. and Schulz, K.V. Polymer. Vol 35, 2108-2116, 1994.

Wortmann, F.J. and Schulz, K.V. Polymer. Vol 36, 2363-2369, 1995.

Yang, H. H., Kevlar Aramid Fiber. John Wiley & Sons, England. 1993.

Zachariades A.E. and Porter. R. S. ed. The Strength and Stiffness of Polymers. Marcel Kekker Inc. 1983.

## APPENDIX A

### Kevlar Aramid Fiber Property Summary

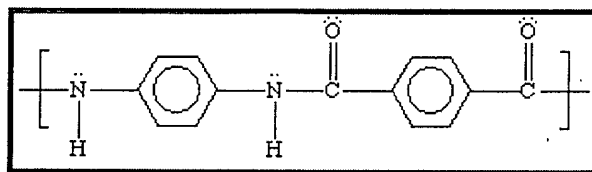
An aromatic polyamide (aramid) fiber [Mark, 1996]

AKA: polyaramide[Mark, 1996]

Poly(p-phenylene terephthalamide) [Mark, 1996]

AKA: Poly(imino-1,4-phenylene iminoterephthaloyl) [Mark, 1996]

A semicrystalline polymer



(internet, same diagram on Mark 171)

### Kevlar 49 properties

[Mark, 1996]

Tg~ 618 K

[Yang, 1993] (Kevlar product comparisons)

Denier/Filament: 1.5

Filament Diameter: .0012 cm

Fiber Cross section: Round

Density: 1.45 g/cm<sup>3</sup>

Yarn elongation: 2.8%

Yarn modulus: 950 gpd

135 GPa

Moisture regain: 3-4%

[Yang 1993] (Comparison of industrial filament yarns)

Tensile Strength: 2758 MPa

Modulus: 124110 Mpa

Elongation to Break: 2.5%

[Yang 1993] (Comparison of high performance fibers)

Max use temperature: 250 C

# Master Creep Sheet

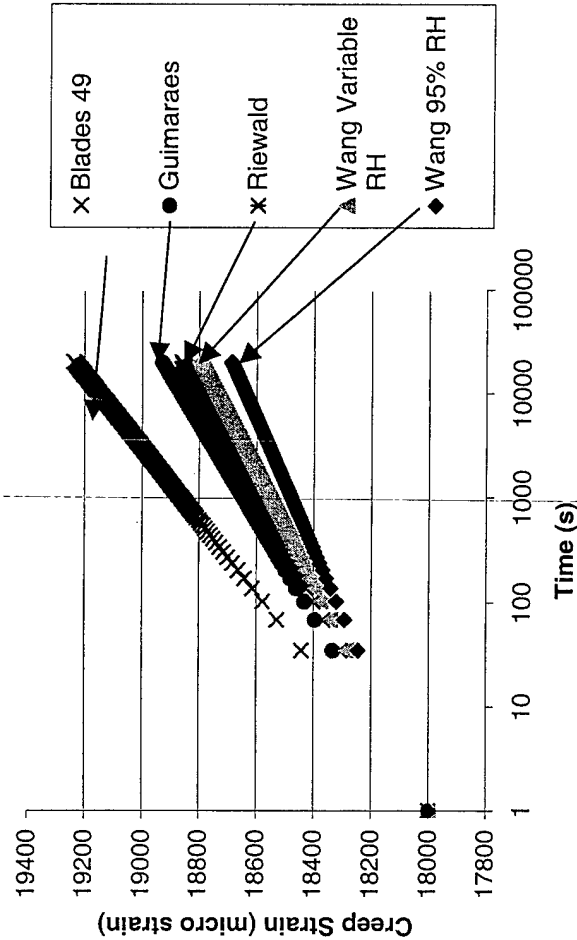
Entries in this sheet filter down to all the other worksheets for comparison purposes.

Time	26280000	S
Time Range	1	to 20000 S
Initial Strain	18000	$\mu\epsilon$
Temp	300	K
% ult. Load		%

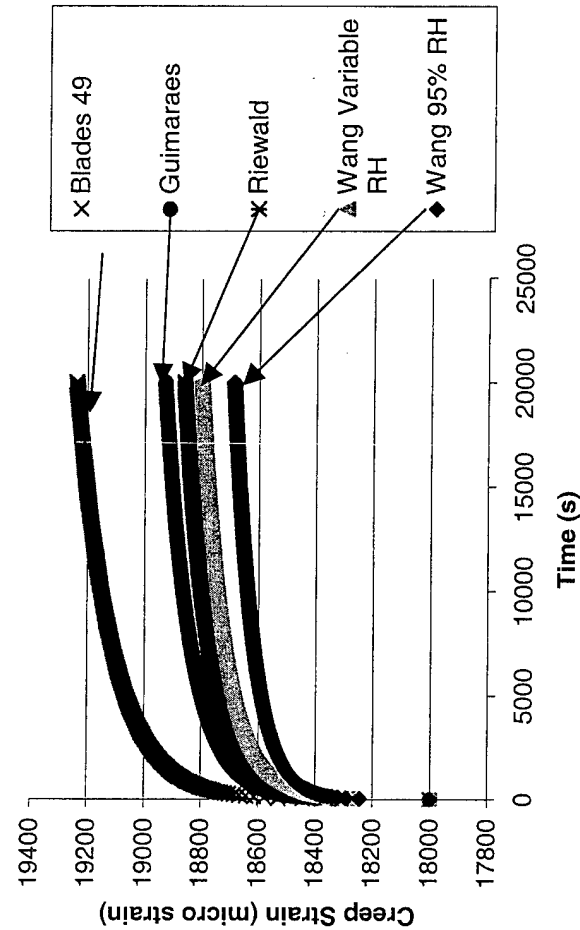
Wang 95%	$\mu\epsilon$
Guimaraes	19185.04
Blades 49	19602.64
Riewald	20136.85
Erickson	19483.93
Duband	0
Lafitte	29129.44
Blades 29	23629.81
	21205.28

Conversion Chart	
50	yrs
5	wks
1	hrs
270	$\mu\epsilon$
1:2	%
0:27	m $\epsilon$
	m $\epsilon$
	%

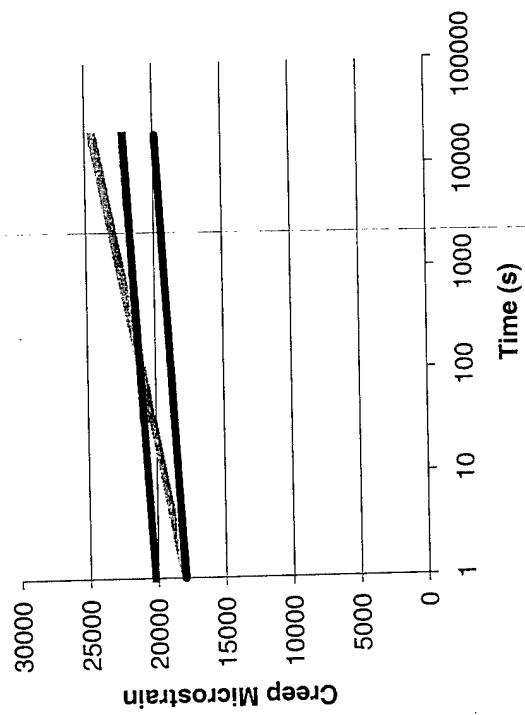
K49 Creep LOG Time Comparison



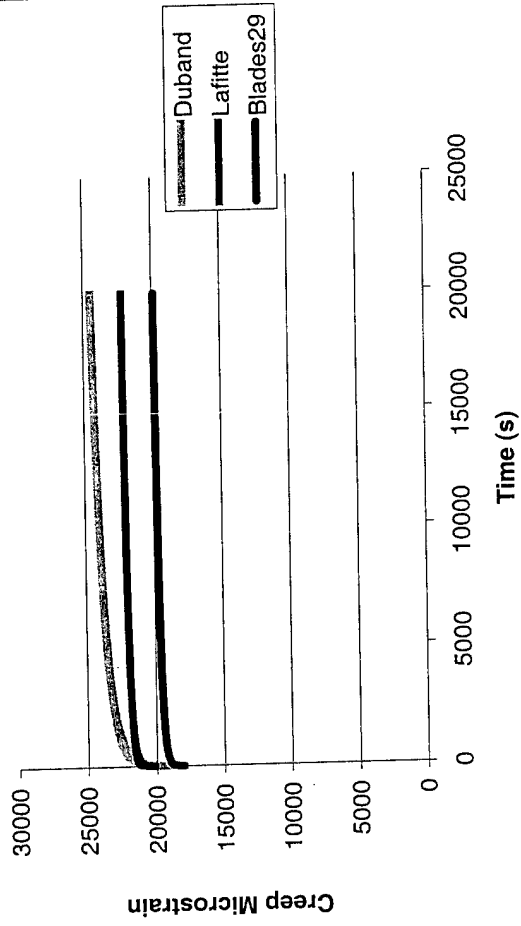
K49 Creep Normal Time Comparison



K29 Log Time Comparison



K29 Normal Time Comparison

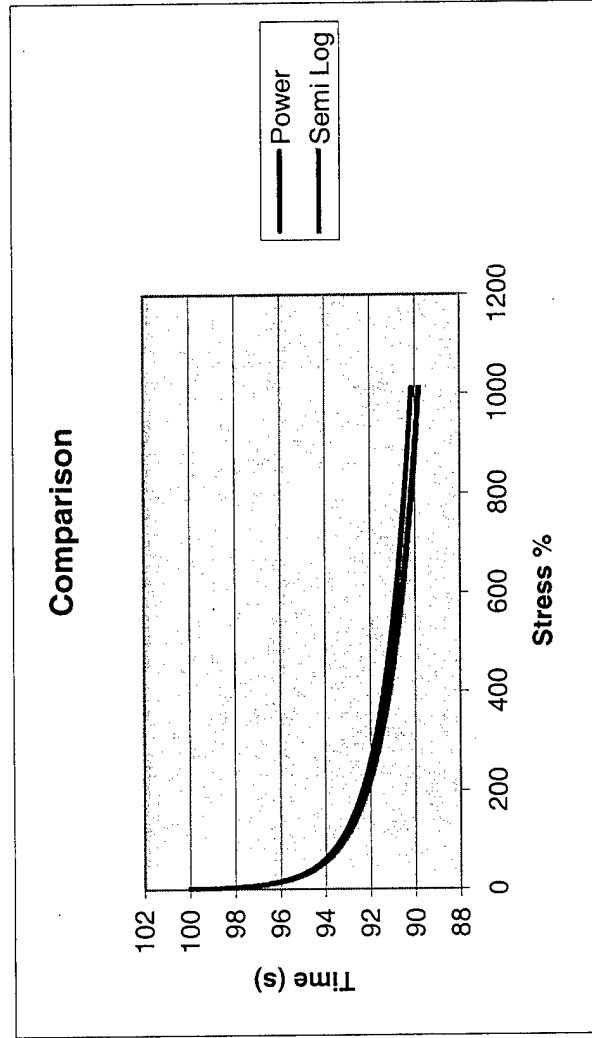


# APPENDIX C Power vs Semi Log Comparison

Time	Power	Semi Log	%err
initial	Beta	Beta	
100	-0.015	-3.394999	
1	100	100	0
2	98.96567	98.978	-0.012467
3	98.36559	98.38017	-0.014831
4	97.94203	97.95601	-0.014271
5	97.61475	97.627	-0.012546
6	97.34816	97.35818	-0.010294
7	97.12332	97.13089	-0.007795
8	96.92898	96.93401	-0.005188
9	96.75788	96.76035	-0.002546
10	96.60509	96.605	9E-05
11	96.46707	96.46447	0.002697
12	96.34125	96.33618	0.005263
13	96.22565	96.21816	0.007779
14	96.11874	96.1089	0.010243
15	96.01932	96.00717	0.012653
16	95.92641	95.91201	0.015009
17	95.83922	95.82263	0.017312
18	95.75708	95.73835	0.019563
19	95.67946	95.65863	0.021763
20	95.60587	95.583	0.023915
21	95.53592	95.51107	0.026019
22	95.46928	95.44248	0.028079
23	95.40565	95.37694	0.030095
24	95.34476	95.31418	0.032069
25	95.2864	95.254	0.034003
26	95.23035	95.19617	0.0359
27	95.17646	95.14052	0.037759

$$\text{SemiLog} \Rightarrow \sigma = \sigma_i + \beta \log(t)$$

$$\text{Power} \Rightarrow \sigma = \sigma_i t^\beta$$



It appears from this analysis that both the power law and a Semi-Log Law will model the scenario in a similar, though not identical fashion. You will note that exact agreement was achieved for time = 10s. But on either side of this mark, there was error. Different Constants are needed for each scenario, which are not obviously related.

## APPENDIX D

### Equipment List

#### *Environmental Control:*

- Electro-tech systems Model 506A Humidity Control Chamber
  - Electro-tech systems Model 514 Automatic Humidity Controller
  - Electro-tech systems Model 562 Ultrasonic Humidification System
- 
- WA Hammond Laboratory Gas Drying Unit with Drierite (Anhydrous  $\text{CaSO}_4$ )
  - Digi-Sense Temperature Controller by Cole-Parmer: Model 89000-00
  - 60 W Soft White Incandescent light bulb in reflective spotlight bell
  - INSTRON Testing Oven Model 3119-409-21
  - UV EPROM Eraser – QUV-T8 by Logical Devices Inc. 115 VAC, 60 Hz, .1 Amp, 6, 8 Watts UV lamp
  - *Additional Heat Lamp capable of reaching 333 K sustained chamber temp*
  - *Additional Cooling source capable of reaching 273 K sustained chamber temp*
  - *System drivers for temperature and humidity cycling*

#### *Data Acquisition:*

- Macintosh Quadra 650 computer
- LabVIEW 5.0.1 by National Instruments 1998
- hp 6216C Power supply at 3V
- hp 3852A Data Acquisition/Control Unit
- hp 44718A 10 Bridge  $350\Omega$  Strain Gage Relay Multiplexer (x2)
- hp 44708A 20 Channel Relay Multiplexer: Thermocouple Compensation Unit
- hp 44705A 20 Channel Relay Multiplexer (used to record humidity data)

- 2 Thermocouples, unknown manufacture
- MM Strain Gages: EA-06-125AC-350 (2.11 gage factor)
- Approx: 24 ft of 3 strand strain gage wire per strain gage

***Fixturing:***

- 5 Load Cells Manufactured at NASA of stainless steel:
  - Heavy Duty Forged 24 inch long, ½"-13 threaded stainless steel bars (4 ea).
  - 5.5 inch square, ½ inch thick plates (2 ea)
  - ½"-13 nuts (12 ea)
  - 1 fixed yoke at bottom with ½ inch threaded bar, extending beyond base plate
  - 1 partially threaded, traveling pin with strain gages (load cell)
  - (initial fixturing) threaded yoke attached to traveling pin
  - ½ inch pins
- Plain Steel Oval Eye Nut 3600#WLL (for fixture revision)

***Loading:***

- INSTRON 4400R
- INSTRON 20,000 lb reversible load cell
- Universal joint with ½ inch pin attachment
- Adapter devices threading onto ½"-13 bar on cells, and ½ inch pins on INSTRON

***Test Specimen Creation:***

- Kevlar Braided B49 16x1420x6 and x4 cordage
- Kevlar Scissors
- Mechanical pencil tip used for splicing
- Yardstick and Sharpie for measurement

## APPENDIX E

### Kevlar Relaxation Test Plan

Russell Fette, 541

23 January 2004

#### Purpose and Objective:

This test plan is being undertaken to experimentally determine the response of Kevlar Braided Cordage under constant strain to a variety of mechanical and environmental variables. It was motivated by a lack of knowledge about this product's response in use in a stress relaxation scenario onboard satellite systems as a tie-down on solar arrays. Stress Relaxation experiments will be performed Kevlar braided cordage in a mechanical laboratory where variables such as temperature, humidity, and preconditioning may be isolated. At the conclusion, a prediction equation or set of equations will be developed from the results. Success will be measured by producing statistically verifiable prediction equations for any of the variables.

#### Test Support:

The testing procedures and equipment for this study are largely without precedent, requiring significant development and raising many accuracy issues. Additional assistance has been sought from varied sources including Mr. Jerry Sterling of Wallops Space Flight, Mr. Doug Bentley of Cortland Cable, and Mr. Michael Viens and Mr. Dave Puckett of NASA Goddard SFC. Primary responsibility for test setup, daily operations, and data analysis reside with Russell Fette, the author of this Test Plan. Technical assistance will be sought primarily from Mr. Dave Puckett. Testing will be performed in the Materials Engineering Branch (Building 30) at NASA Goddard SFC, using branch resources. The majority of fixturing, equipment, and test material is already in place and available. New resource acquisition is expected to be minimal. Possible exceptions include: new load cells relaxation cells, additional forms of Kevlar product, strain gages and wire, heat lamps, and fixture grip alternatives. A list of specific equipment used is included as Attachment A to this Test Plan.

#### Timeline and Schedule:

Table 1: Kevlar Schedule

Kevlar Relaxation Study Timeline and Schedule		
Start Date	End Date	Task/Event
5-Aug-2003	3-Oct-2003	Literature Review and Report
24-Sep-2003	3-Oct-2003	Design of Experiments
7-Oct-2003	14-Oct-2003	Test Specimen creation and verification
14-Oct-2003	21-Oct-2003	Test Setup and Calibration
22-Oct-2003	18-Dec-2003	Testing with Initial Setup, Phase 1, Time section
16-Dec-2003	18-Dec-2003	New Test Setup
18-Dec-2003	11-Feb-2004	Testing with Second Setup, Phase 1, Time section
11-Feb-2004		Choose path of experimentation
11-Feb-2004	1-Jun-2004	Conclude Phase 1 testing
1-May-2004	1-Jul-2004	Perform Phase 2 testing if required
1-Jun-2004	1-Jul-2004	Data Analysis and Statistical Conclusions
1-Jul-2004	1-Aug-2004	Complete Thesis Conclusions and report
1-Aug-2004	1-Sep-2004	Complete Thesis Revisions and Present

## Description of the Test Article:

Conversations with Mr. Michael Viens and Mr. Dave Puckett, along with correspondence with Mr. Jerry Sterling at Wallops Space Flight, and Doug Bentley of Cortland Cable led to the development of the final test specimen buildup for the braided cord. Splicing was the only feasible method to provide universal loading on all fibers and high strength capability. This was proven through testing configurations to failure such as knotted and various length splices. The dimensions were designed to give the minimum splice length without failure by pullout with the maximum gage of plain cordage between the splices. The overall length was limited by the two-foot long relaxation cells to be used. Each specimen is made from a 26-inch length of cord, which is given a four-inch eye splice with a one-inch long flat eye. The specimens are then a total of 16 inches long, as pictured below.



Figure 1: Dimensioned Picture of Test Specimen

However, before the 4<sup>th</sup> test run, the middle section was reduced from six to five inches due to a change in the fixture dimensions. The new overall length was 15 inches, as the spliced sections did not change.

After experimentation with the splice length and development of the final test specimen, a series of tensile tests were performed on the 2 types of cord to be used. They were braided by Cortland cable, and designated B49 16x1420x6, or B49 16x1420x4. This refers to Kevlar 49 material braided into a 16-strand braid of 1420-denier yarn with either 6 or 4 lines per strand. The x6 version therefore has 50% more material than the x4 variety. The strength testing was intended to determine a baseline ultimate load since the literature review demonstrated that a purely theoretical calculation did not follow actual material values closely. The results of these strength tests are summarized in the table below.

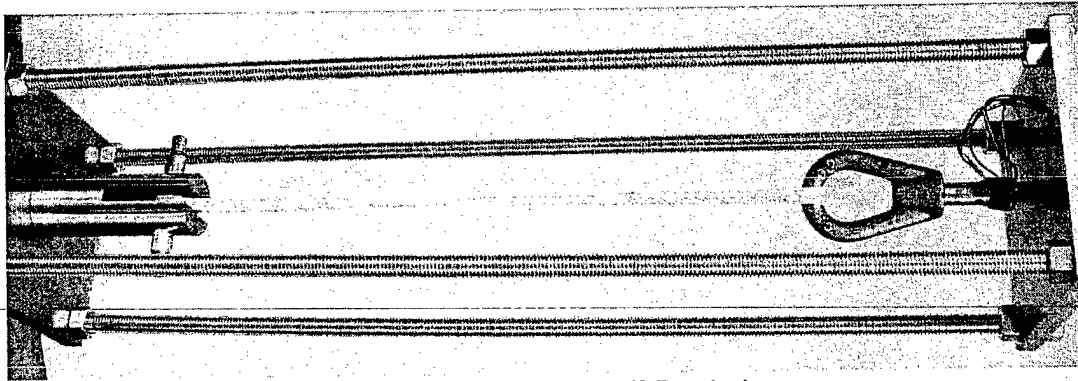
Cordage	Failure lbs	Failure Mode
B49 16x1420x6	4400	Loop base
B49 16x1420x6	4500	Splice transition
B49 16x1420x4	3175	Splice transition
B49 16x1420x4	3465	Splice transition
Performed on INSTRON 4485 at 0.5 in crosshead speed to specimens with twin 4 inch eye splices		

Table 2: Summary of Strength Testing

## Instrumentation Plan:

The test fixtures used will be referred to as relaxation cells, or cells. They were left over from a previous Kevlar relaxation study done at NASA Goddard, and proved to be ideal for this testing with minor modifications. The cells are stainless steel, consisting of four, ½"-13 threaded bars two feet long, with a ½" stainless steel plate bolted to each end. Through a center hole in each plate, a yoke is attached. The bottom yoke is fixed, and the top slides freely through the

whole until stopped by a nut on the threaded bar holding the yoke. Half-inch pins through the eye splice grip the specimens. The setup of the relaxation cell is pictured below.



*Figure 2: Relaxation Cell Depiction*

Due to the high loads to be employed, the load cells available in the lab were unacceptable. Rather than purchase new load cells, the tensioning bar was fitted with strain gages and calibrated for load. A Micro Measurements EA-06-125AC-350 gage was attached to each side of the smooth steel bar and aligned by eyesight to be along the tensile axis.

During initial attempts to calibrate the system, each cell was loaded with a dummy specimen and then loaded into an INSTRON 4485 mechanical testing machine. They were tensioned at 0.5-in/min-crosshead speed up to 80% of the load seen in the strength tests. This data was then plotted against the average of the two strain gages. The resulting curve was almost perfectly linear, and the constant derived from the slope was used in a LabVIEW program to convert the strain from the gages to load. However, it was necessary to repeat this loading sequence three to four times to obtain consistency in the results. This has been noted by Mr. Puckett before and may be a settling of the strain gage. In the end, the calibration constant was set during the actual specimen loading process to minimize variations caused by bending and the test environment.

After the first three test runs, erratic data motivated a revision of the test setup in order to remove any possibility of bending affecting the fixturing. Two more strain gages were added to the traveling bar so that a total of four were present at 90 degree intervals around it. The strain from all four was averaged to remove the effects of bending and report the purely tensile loads. Also, the traveling yoke was replaced with a single cast eye nut, pictured below. Each was polished by hand with the assistance of Mr. Dewey Dove to prevent abrasion of the cords.

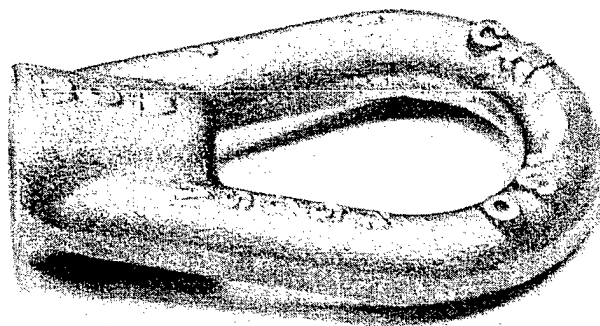


*Figure 3: Cast eye bolts.*

### Test Setup:

In order to precisely control humidity and temperature, which have been shown to have direct effects on the tension of Kevlar, a sealed Plexiglas test chamber was employed. A simple incandescent light bulb with a temperature controller was used as a heat source, which was able to consistently hold the test chamber with  $1/10^{\text{th}}$  of a degree C for temperatures slightly above room temperature. A humidifier, de-humidifier, and controller held the chamber within 1% relative humidity while the chamber was closed. *During testing for the CTE and CME, additional temperature control equipment will be necessary, as well as additional operative software to cycle the variables according to a ramp time.* A list of the specific equipment can be found at the end of this section. A photograph of the environmental chamber with a relaxation test running is shown below.

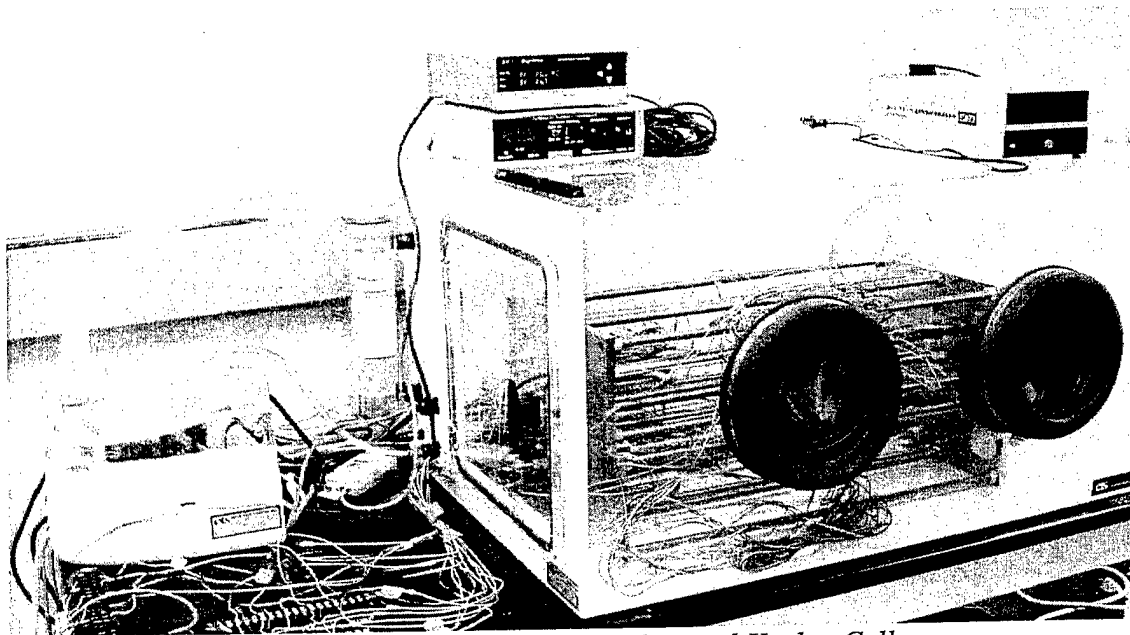


Figure 4: Environmental Chamber and Kevlar Cells.

### Data Acquisition:

A Macintosh computer running LabVIEW 5.0.1 recorded the data through a Hewlett Packard Data Acquisition/Control Unit. The data from four strain gages was averaged for each unit and multiplied by a calibration factor. This was recorded along with room temperature, chamber temperature, chamber relative humidity, and a time stamp. Initially these were recorded approximately 10 seconds apart. After at least one hour of relaxation, the time between data points was increased, up to 600 seconds.

### Preconditioning:

Specimens may be preconditioned to achieve uniform moisture content prior to testing in an INSTRON test oven at specified temperatures and times prior to employment. They are sometimes exposed to UV light using UV EPROM Eraser. Preloading/relaxation is done within the test-cells on an INSTRON 4400R.

## Test Procedures:

This section contains the typical loading procedure used for testing. Variations and specific values are recorded with individual tests. This information is found as Attachment B to this test plan. This is performed in an INSTRON 4400R. A photograph of the cell and specimen loaded into the INSTRON to begin a test run is seen below.

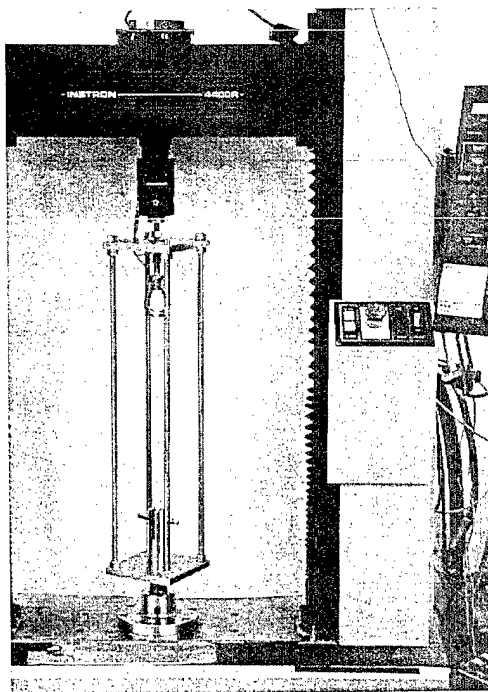


Figure 5: Specimen loading in INSTRON.

### Procedure:

- 1) Create, randomly select, and mark specimens
- 2) Perform any preconditioning
- 3) Check that plates are parallel with level
- 4) Tighten all fixture nuts
- 5) Remove Kevlar specimen from preconditioning oven and install
- 6) Attach adapter grips to threaded center bars of cell and insert into INSTRON
- 7) Manually tension to calibration load.
- 8) Set to cycle between  $+1/-1$  lb of calibration load at 0.02 in/min crosshead speed.
- 9) Calibrate in LabVIEW
- 10) Set crosshead stop at pretension load and pull at 0.2 in/min to pretension load
- 11) Relax at pretension load for specified time
- 12) Re-tension to final load at 0.02 in/min
- 13) Tighten fixture load nut as much as possible with minimal twisting of yoke
- 14) Unload crosshead manually
- 15) Remove cell and place into environmental chamber
- 16) Repeat as necessary for other fixtures
- 17) Close environmental chamber and monitor

## **Data Analysis Plan:**

Data from each test has been analyzed initially using Microsoft Excel. The data is normalized for time, and two slope values are recorded: pretensioning (30 min relax period during loading) and relaxation. Excel fits them according to a best-fit log equation, and the R squared value is recorded as well. Finally, the data is graphed along with all the environmental variables to search for anomalies caused by the environment. Recorded values are stored together in a separate Spreadsheet for easy comparison.

Due to the effects of temperature on the lead wires outside the chamber, it may become necessary to trim out this effect using room temperature information recorded with the test. This may be analyzed in MINITAB. Also, statistical results for the overall testing will be done in MINITAB.

## **Reporting Requirements:**

Two similar, but separate reports are required at the completion of this project. One is a formal NASA report on the testing to be submitted to Mr. Michael Viens for review and filing. The second is a Master's Thesis Report to be submitted orally and with a written report before a panel including Mr. Viens, Dr. Sarkani, and one other individual. The following is from notes during a conversation with Dr. Sarkani reflecting guidance for the thesis.

Basic outline of Master's Thesis

- 1) Introduction: 3-5 pages
- 2) Background: 6-10 pages
- 3) Problem Statement (what are you doing): 6-10 pages
- 4) Results and Analysis: 6-10 pages
- 5) Conclusions: 2 pages
- 6) Future Direction: ½ page

75-80% of this is prior knowledge that you have reported after research  
25-20% is new knowledge that you have obtained

## APPENDIX F

### Collection of Test Plots

#### CONTENTS

- Kevlar Testing Conditions
  - Steel Bar Proof Test
  - Primary and Secondary Relaxation
- 
- Kevlar Test 1-6

#### NOTES

Specific Information on each test run is provided as the first page. All Plots are on a Logarithmic Time Scale. The Large Diameter cordage has 50% more material than the Small Diameter, and thus 50% greater cross sectional area, and thus:

*Large Diameter Cord has 2/3 of the stress of the Small Diameter cord*

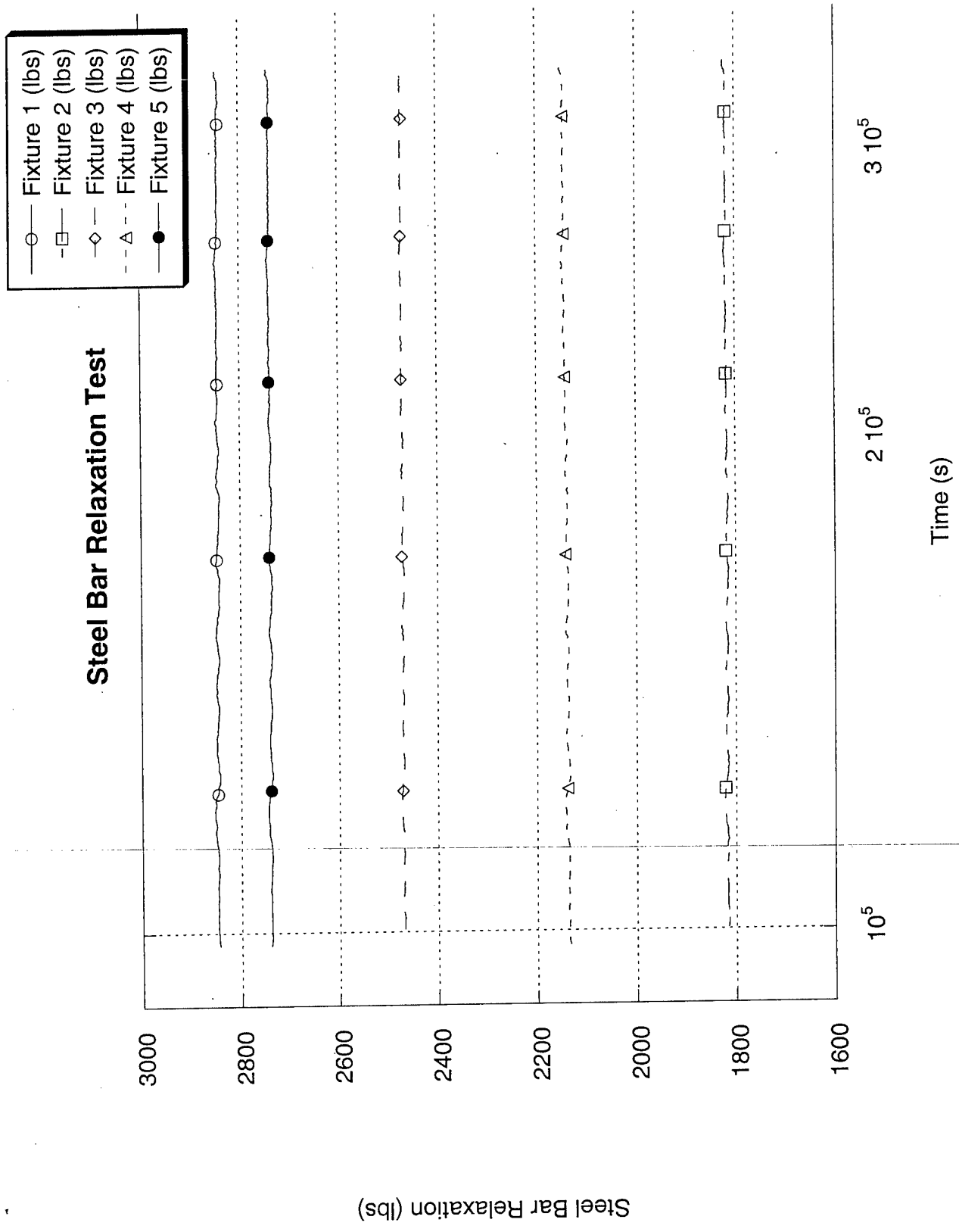
- Steel Bar Proof Test: A chart showing the results of testing steel bars in place of the Kevlar strands to validate the test fixturing. Notice the lines are generally linear.
- Tests #1,2,3,4,6 are pictured on the same scale (500 lbs) and range (1900-2400 lbs)
- Kevlar Relaxation #5 has the same scale (500 lbs) but a different range (1200-1700 lbs)

## Kevlar Testing Conditions

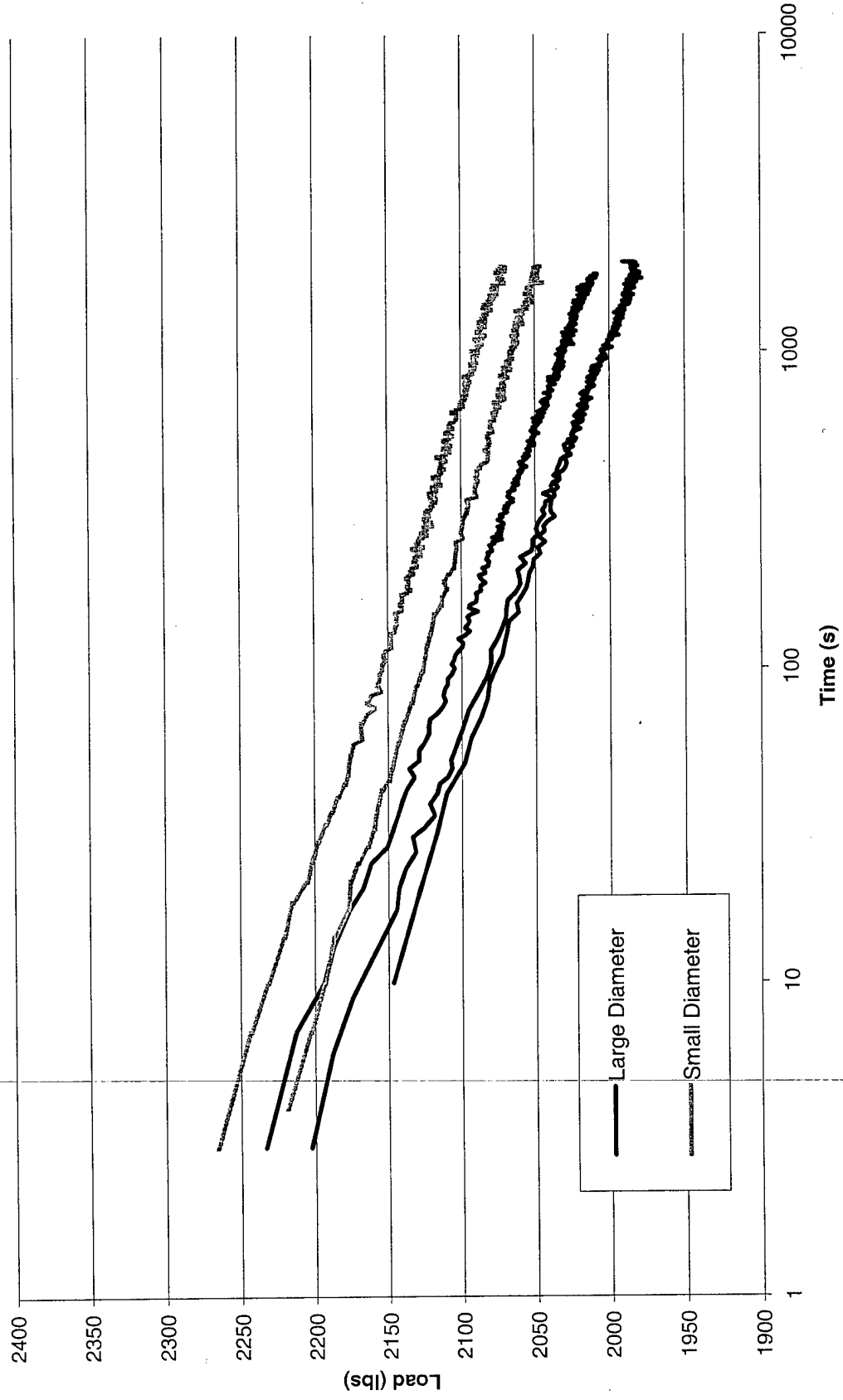
	Date	Product	Setup	Pretensioning		Preconditioning		Temp	Humidity	Initial Load	Total Time	Cal	other
				load (lbs)	time (min)	temp (K)	time (hr)	(K)	(%)	(lbs)	(d)		
1.1	22-Oct	K49-6	2gagē yk	2250	30	333	20	299.85	60	2250	19.1		
1.2	22-Oct	K49-6	2gagē yk	2250	30	333	20	299.85	60	2250	19.1		
1.3	22-Oct	K49-6	2gagē yk	2250	30	333	20	299.85	60	2250	19.1		
1.4	22-Oct	K49-4	2gagē yk	2250	35	333	20	299.85	60	2250	19.1		
1.5	22-Oct	K49-4	2gagē yk	2250	30	333	20	299.85	60	2250	19.1		
2.1	10-Nov	K49-6	2gagē yk	2250	30	333	20	299.85	60	2250	22.8		
2.2	10-Nov	K49-6	2gagē yk	2250	30	333	20	299.85	60	2250	22.8		
2.3	10-Nov	K49-6	2gagē yk	2250	30	333	20	299.85	60	2250	22.8		
2.4	10-Nov	K49-4	2gagē yk	2250	30	333	20	299.85	60	2250	22.8		
2.5	10-Nov	K49-4	2gagē yk	2250	30	333	20	299.85	60	2250	22.8		
3.1	3-Dec	K49-6	2gagē yk	2250	26	333	20	299.85	60	2250	7.0	5.53	
3.2	3-Dec	K49-6	2gagē yk	2250	25	333	20	299.85	60	2250	7.0	5.63	
3.3	3-Dec	K49-6	2gagē yk	2250	25	333	20	299.85	60	2250	7.0	5.8	respiced at top
3.4	3-Dec	K49-4	2gagē yk	2250	75	333	20	299.85	60	2250	7.0	5.75	
3.5	3-Dec	K49-4	2gagē yk	2250	25	333	20	299.85	60	2250	7.0	5.83	
4.1	19-Dec	K49-6	4gagē eye	2250	30			299.85	60	2250	17.3	5.374	
4.2	19-Dec	K49-6	4gagē eye	2250	30			299.85	60	2250	17.3	5.388	
4.3	19-Dec	K49-6	4gagē eye	2250	30			299.85	60	2250	17.3	5.438	
4.4	19-Dec	K49-4	4gagē eye	2250	30			299.85	60	2250	17.3	5.291	lots of yarns cut
4.5	19-Dec	K49-4	4gagē eye	2250	30			299.85	60	2250	17.3	5.265	Chamber not closed between fixture loading, humidity issues caused useful data collection to be delayed 1 day
5.1	12-Jan	K49-6	4gagē eye	1500	20			299.85	60	1500	14.8		
5.2	12-Jan	K49-6	4gagē eye	1500	20			299.85	60	1500	14.8		
5.3	12-Jan	K49-6	4gagē eye	1500	35			299.85	60	1500	14.8		
5.4	12-Jan	K49-4	4gagē eye	1500	20			299.85	60	1500	14.8		
5.5	12-Jan	K49-4	4gagē eye	1500	20			299.85	60	1500	14.8		

## Kevlar Testing Conditions

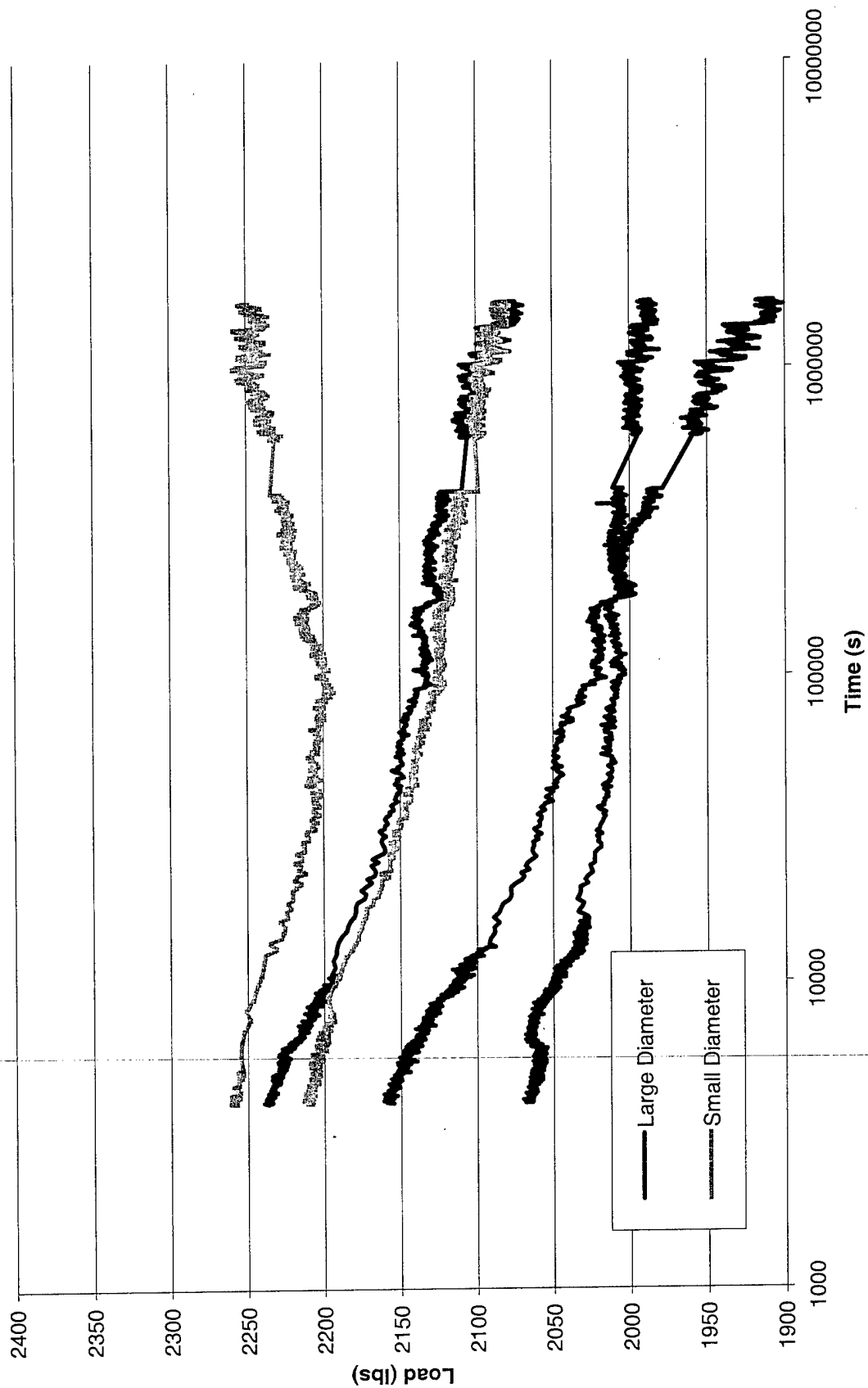
	Date	Product	Setup	Pretensioning		Preconditioning		Temp	Humidity	Initial Load	Total Time	Cal	other
				load (lbs)	time (min)	temp (K)	time (hr)	(K)	(%)	(lbs)	(d)		
6.1	28-Jan	K49-6	4gagē eye	2250	30	333	20	300	60	2250	63.3	5.5	specimens attached to fixture and allowed to cool completely before test began
6.2	28-Jan	K49-6	4gagē eye	2250	30	333	20	300	60	2250	63.3	5.5	
6.3	28-Jan	K49-6	4gagē eye	2250	30	333	20	300	60	2250	63.3	5.55	
6.4	28-Jan	K49-4	4gagē eye	2250	30	333	20	300	60	2250	63.3	5.44	
6.5	28-Jan	K49-4	4gagē eye	2250	30	333	20	300	60	2250	63.3	5.5	



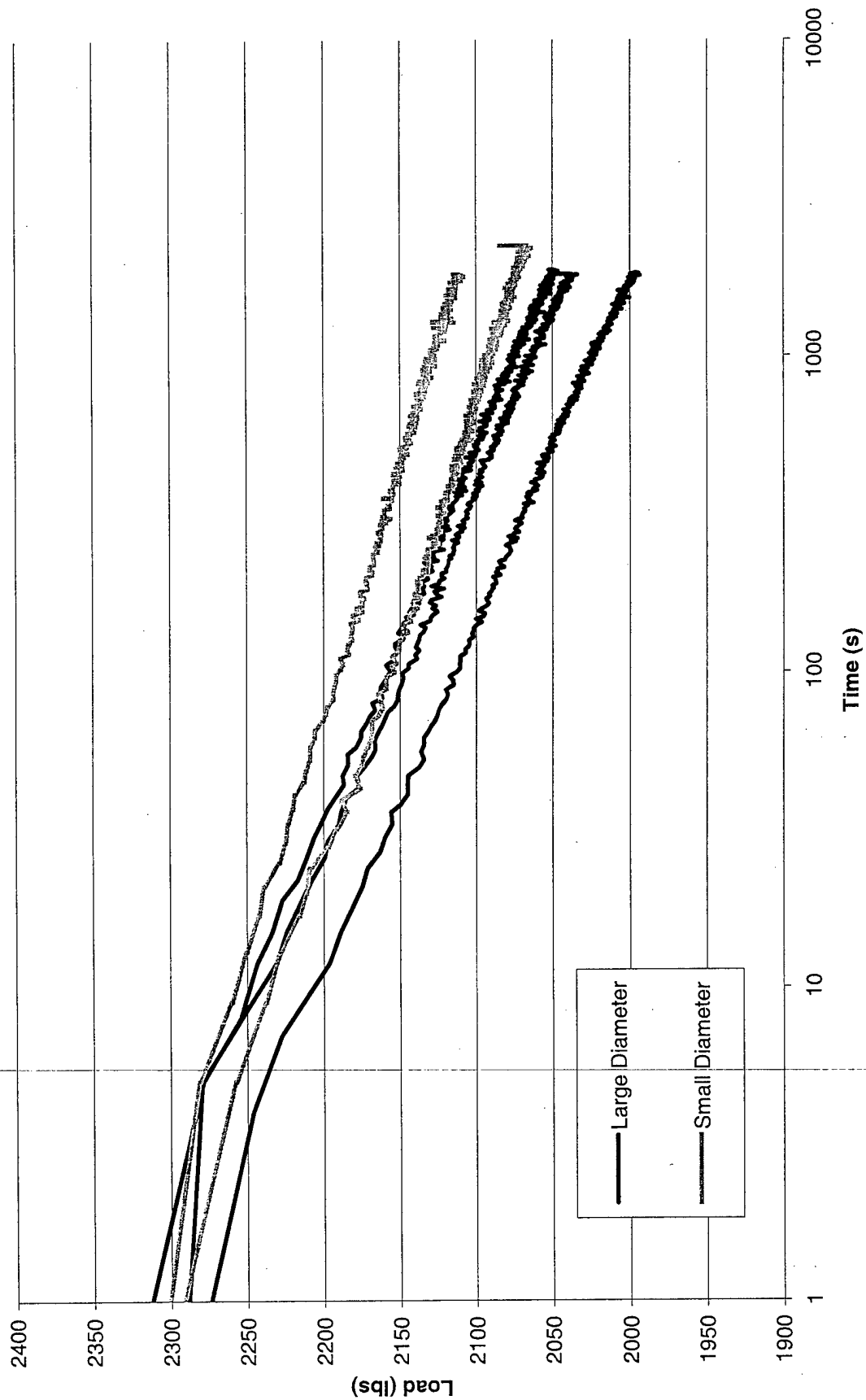
# Primary Relaxation Kevlar Test 1



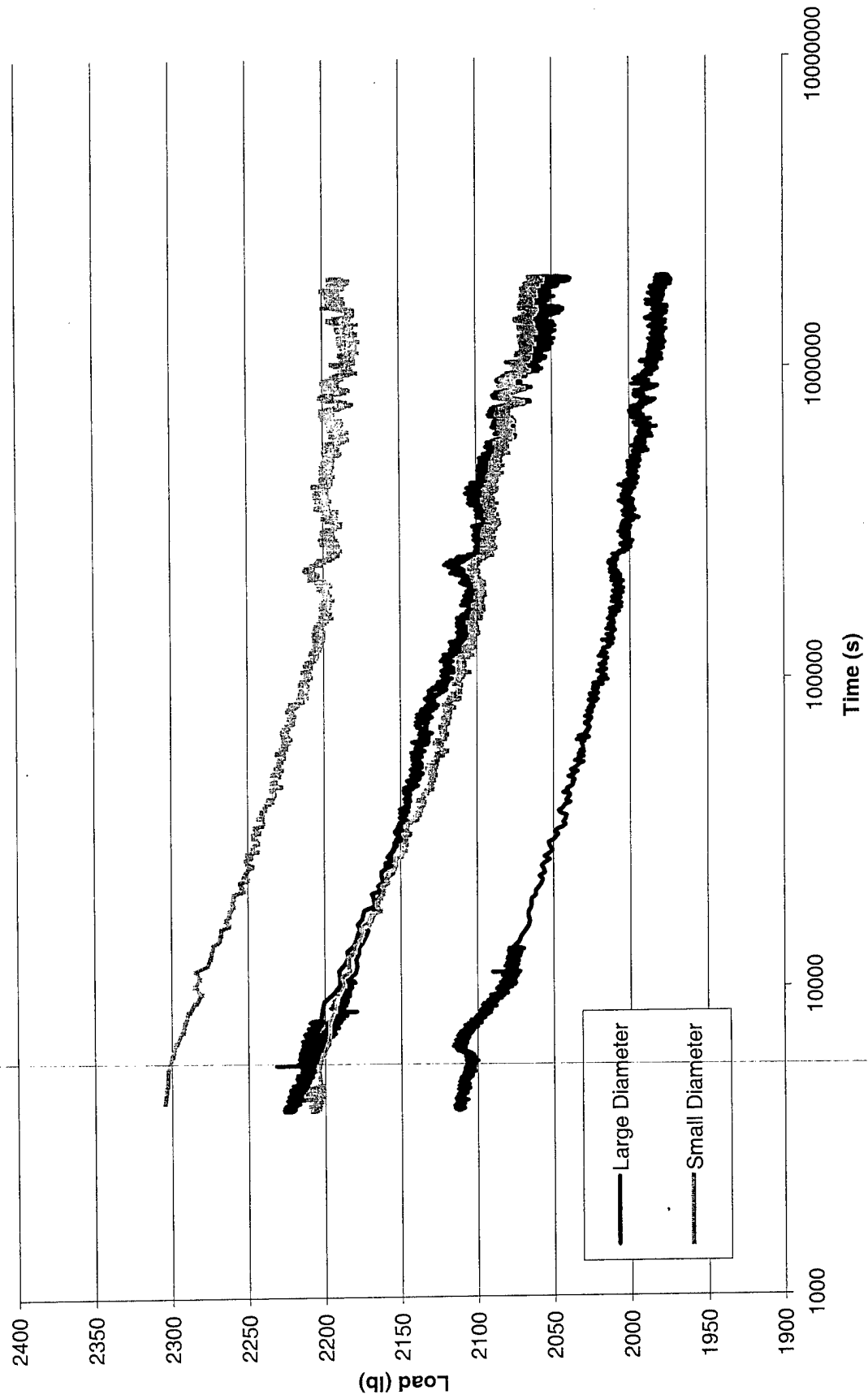
# Secondary Relaxation Kevlar Test 1



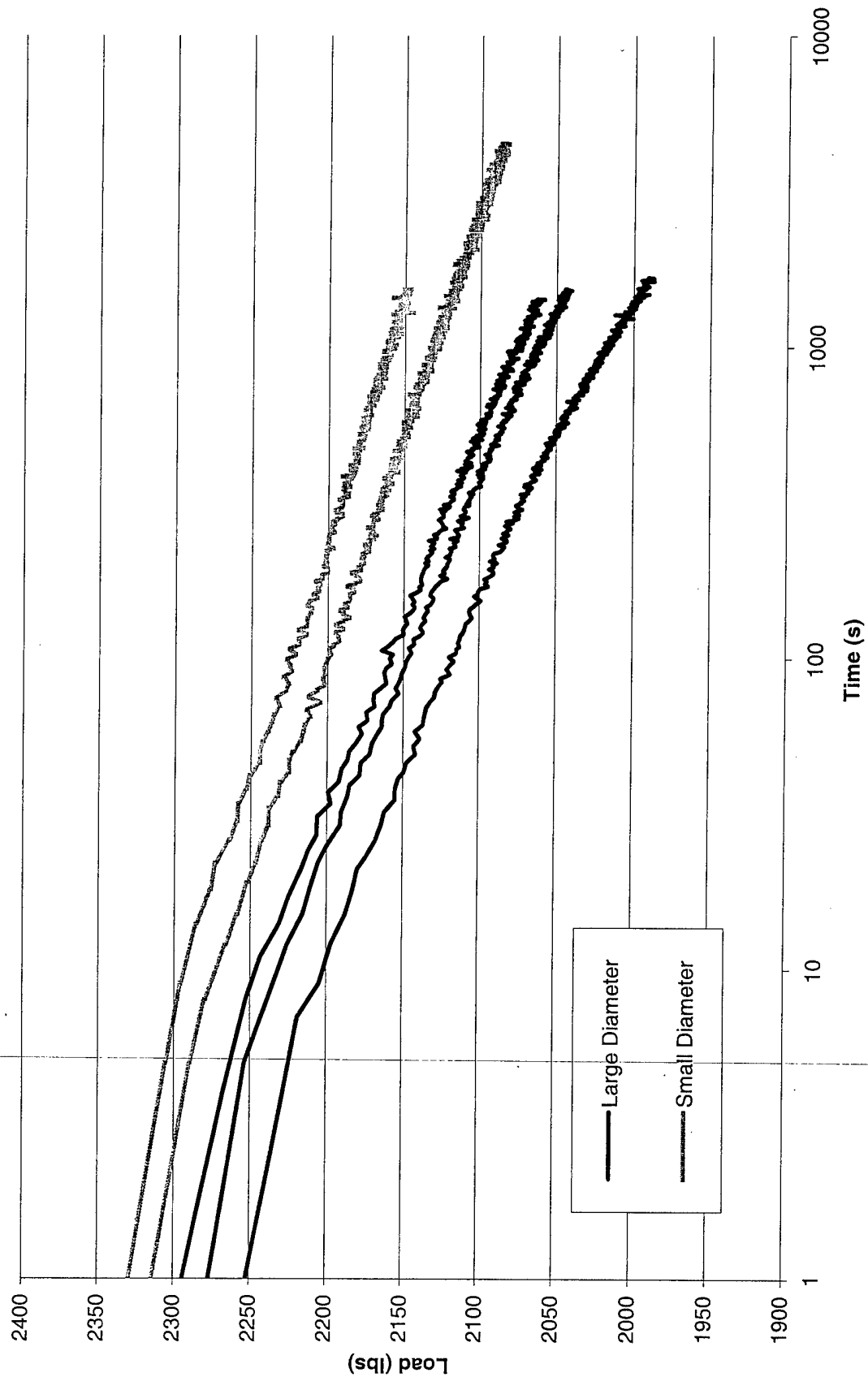
# Primary Relaxation Kevlar Test 2



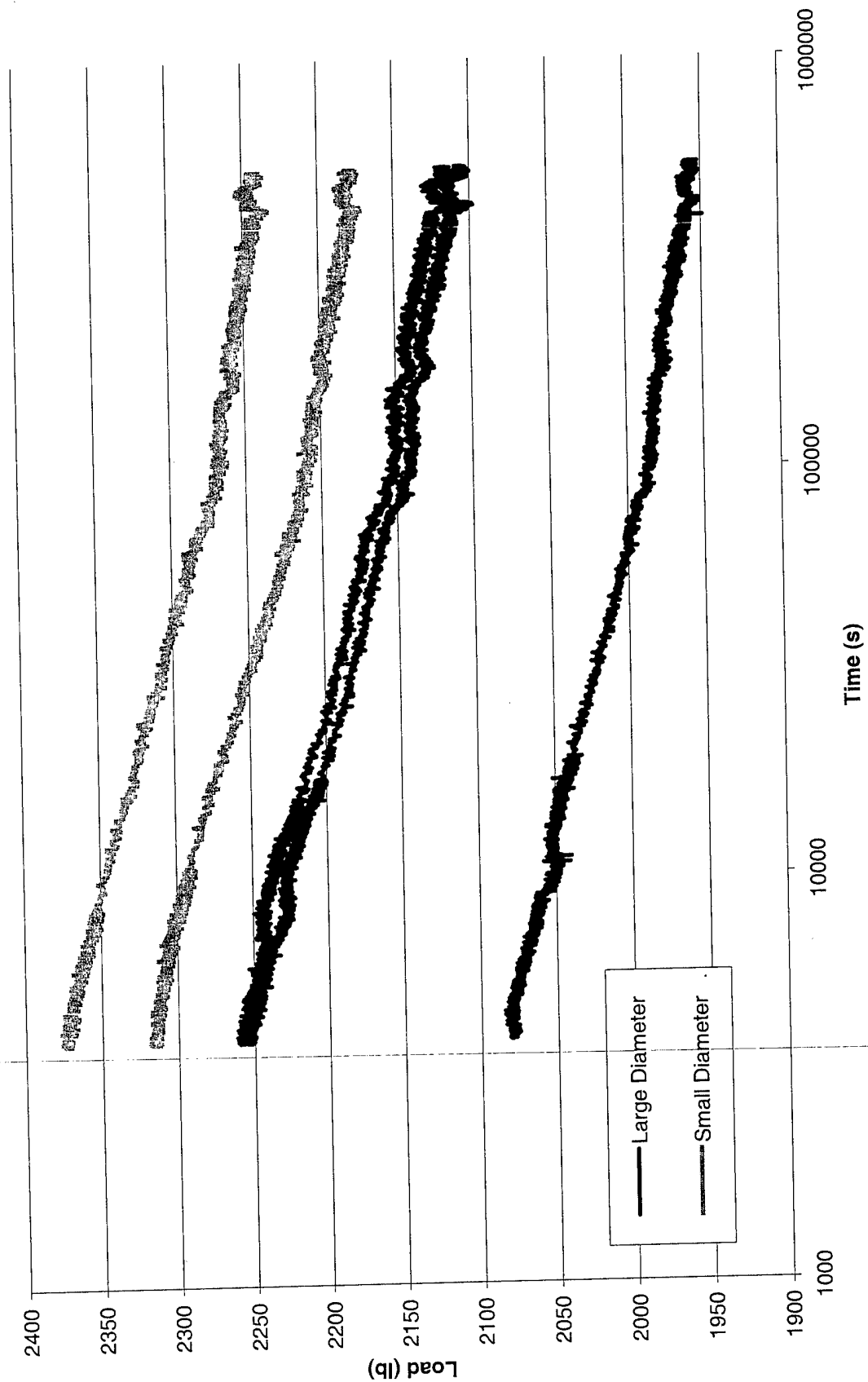
# Secondary Relaxation Kevlar Test 2



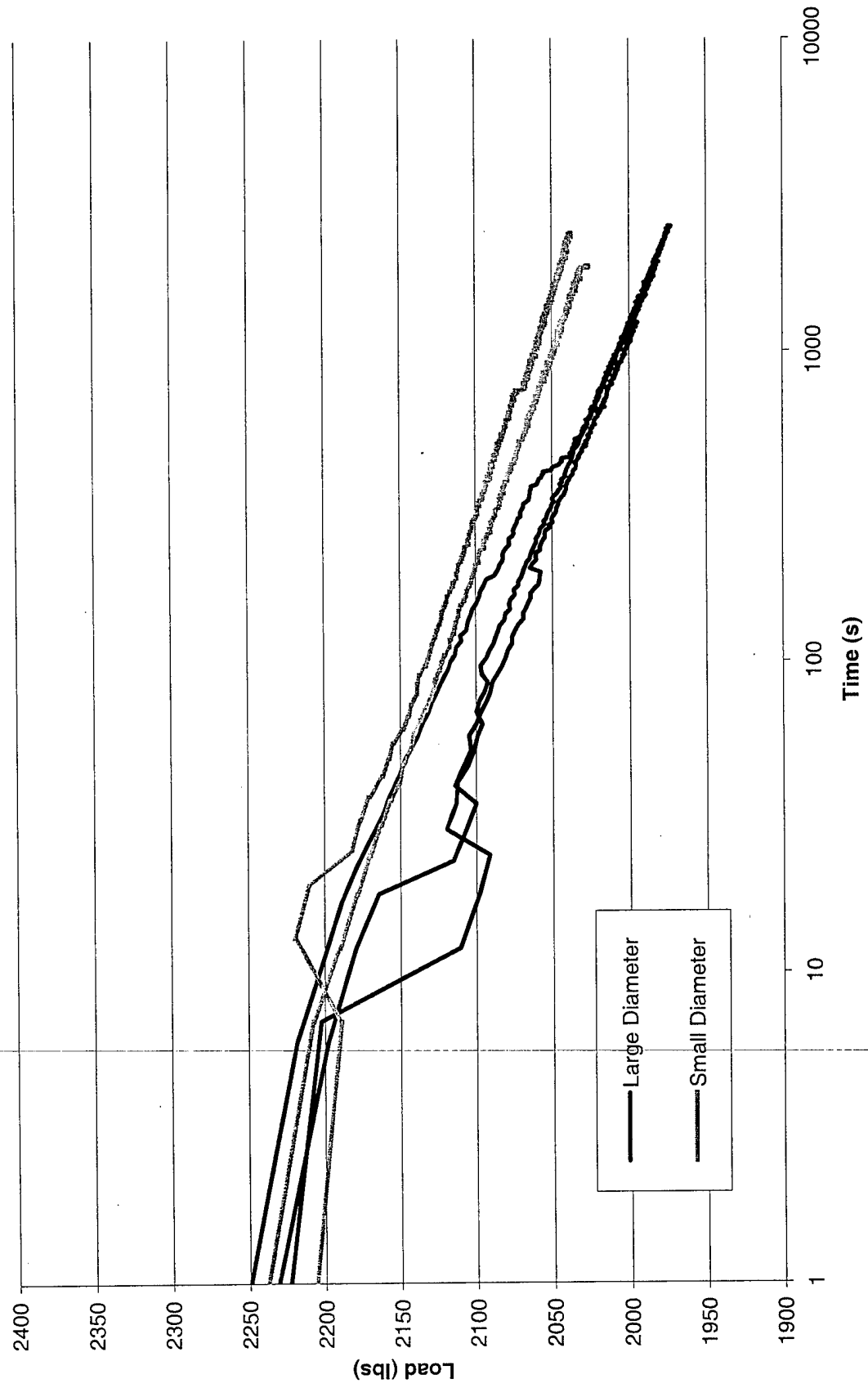
### Primary Relaxation Kevlar Test 3



### Secondary Relaxation Kevlar Test 3

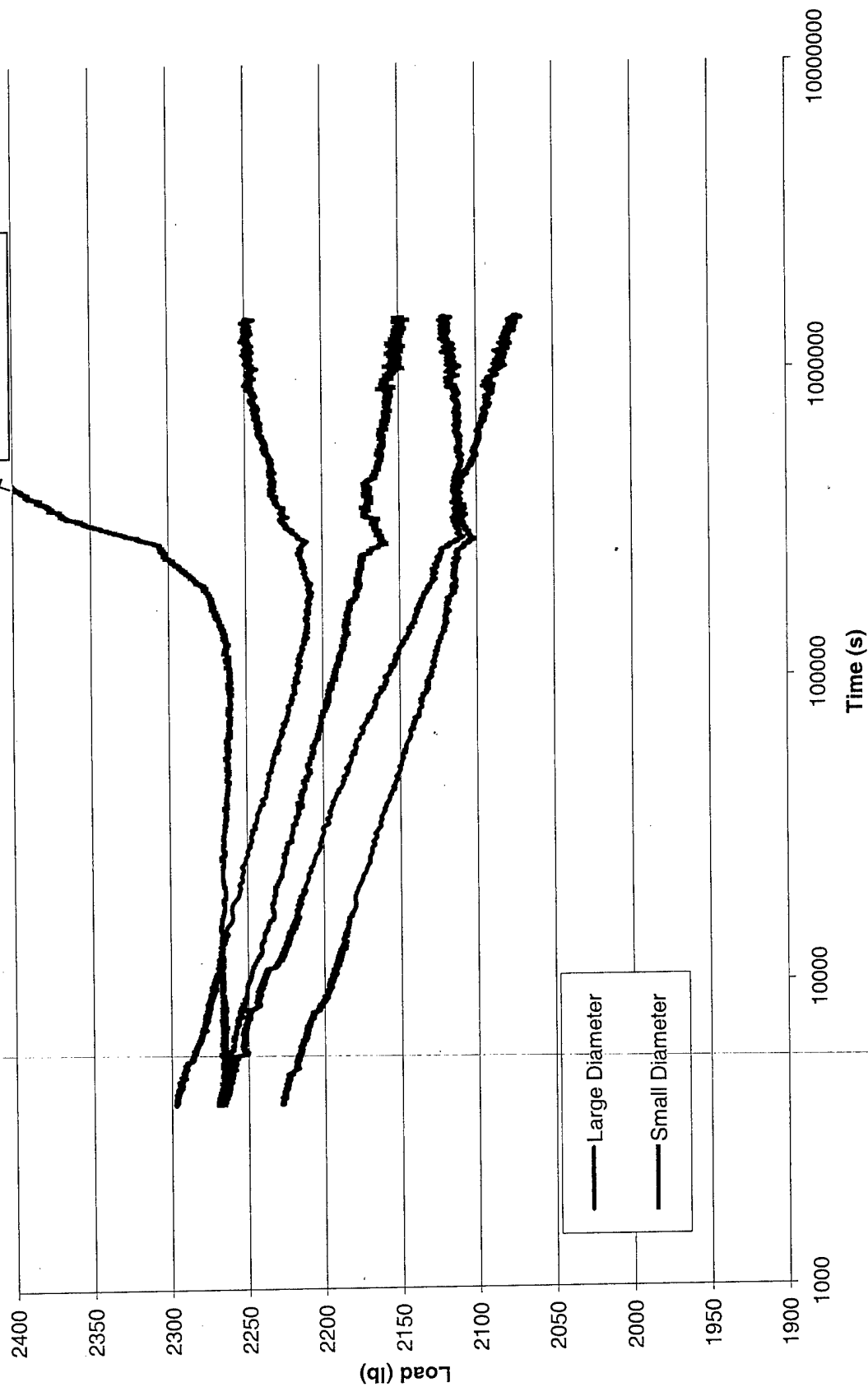


# Primary Relaxation Kevlar Test 4

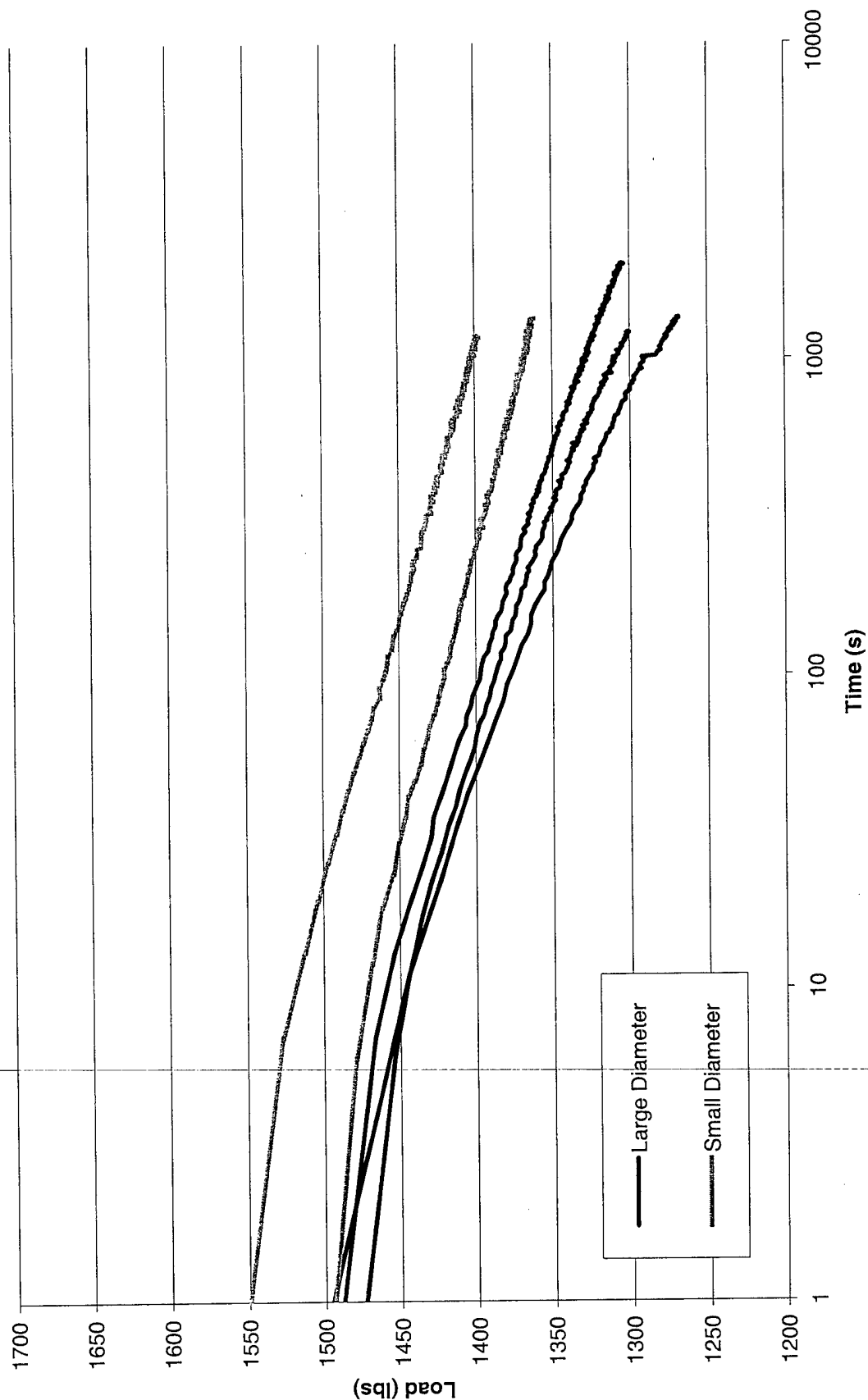


# Secondary Relaxation Kevlar Test 4

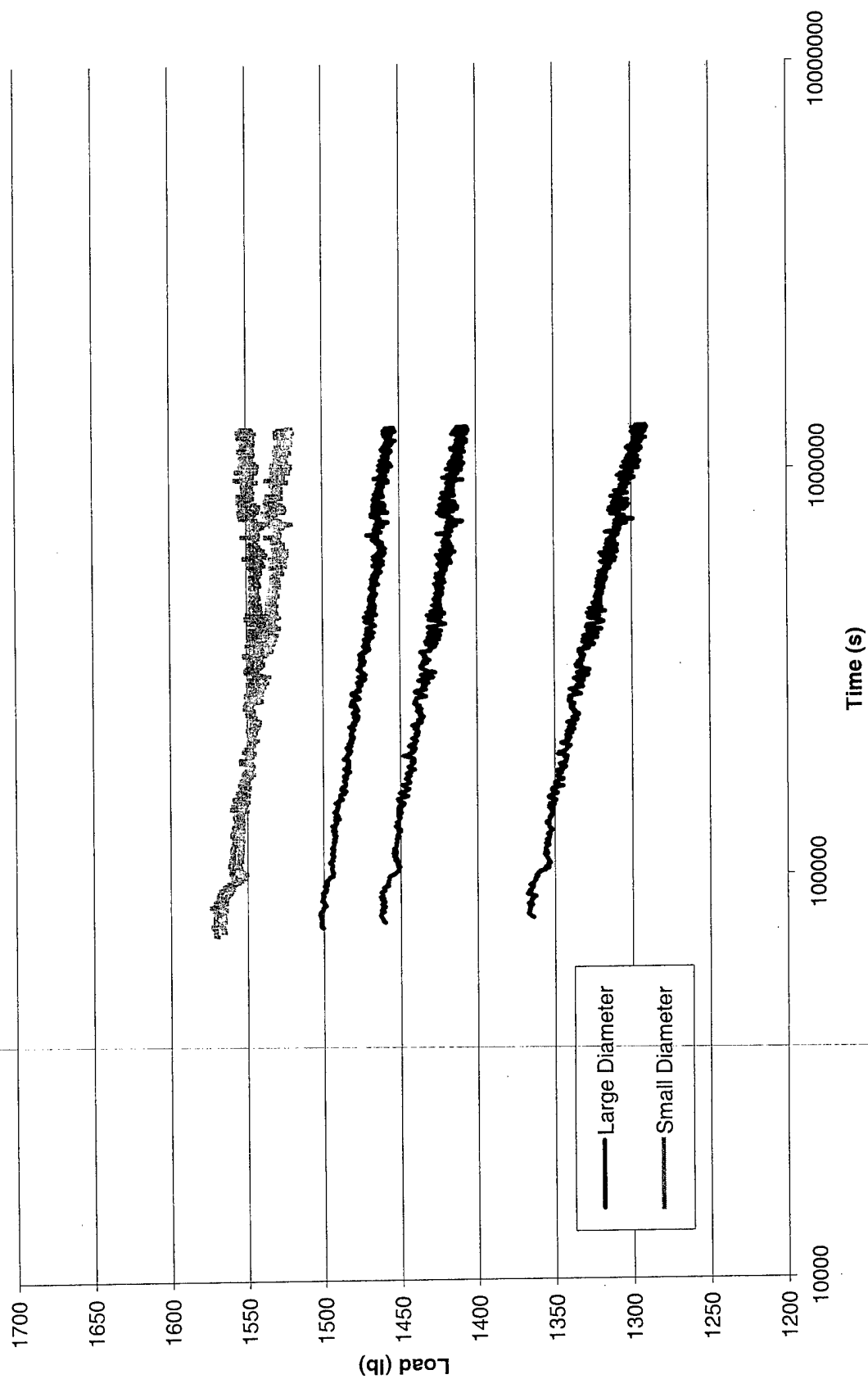
Continues up until test termination



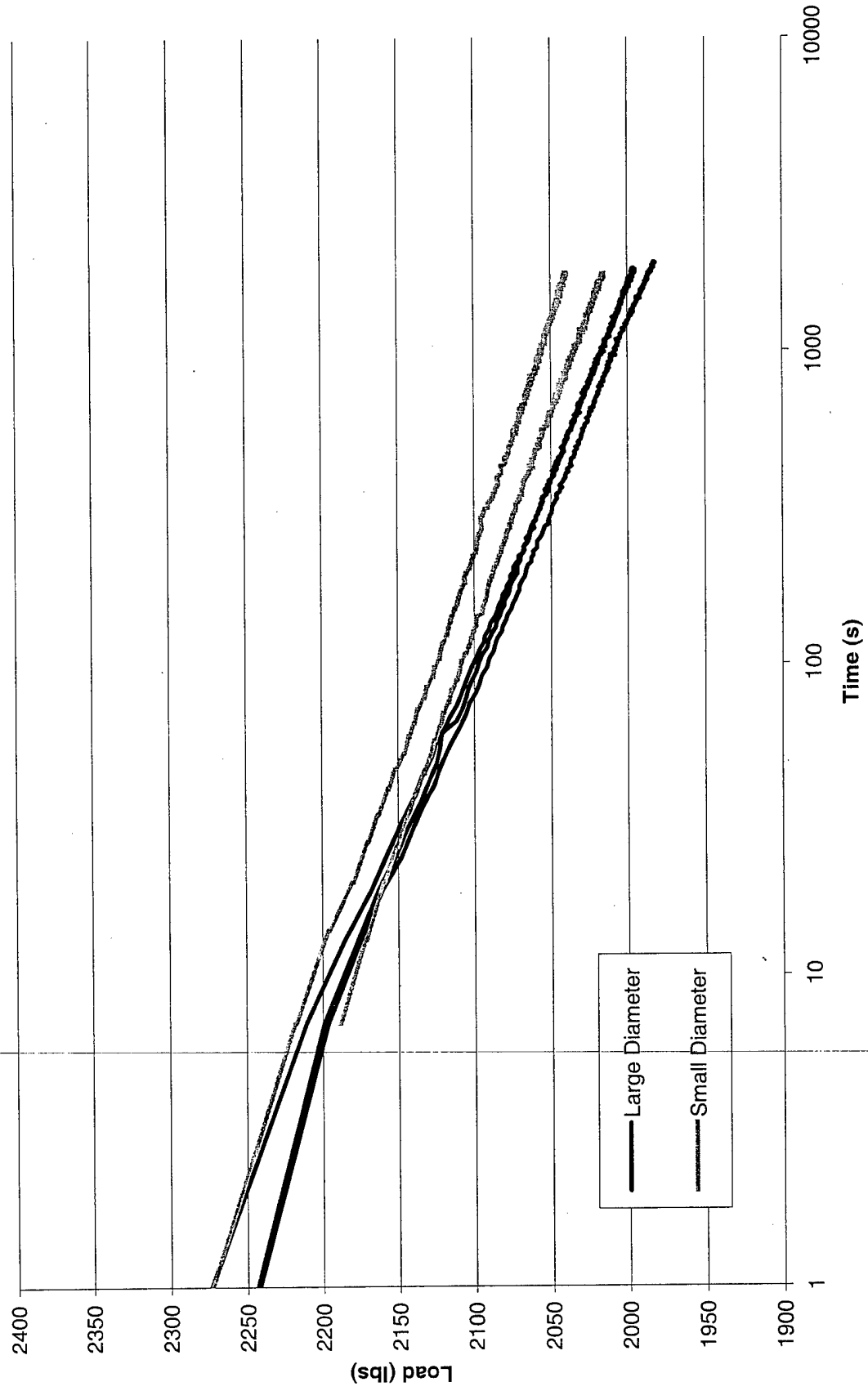
# Primary Relaxation Kevlar Test 5



# Secondary Relaxation Kevlar Test 5



# Primary Relaxation Kevlar Test 6



# Secondary Relaxation Kevlar Test 6

